Learning Task-Sufficient World Models by Synergizing Agentic Exploration and Structured Modeling

Fan Feng [*1 2] **Yujia Zheng** [*3] **Minghao Fu** [1] **Yongqiang Chen** [2 3] **Guangyi Chen** [2 3]
Kevin Murphy [4] **Biwei Huang** [1] **Kun Zhang** [2 3]

Abstract

Learning and planning in imagination using world models provides an effective paradigm for training agents for decision-making. However, existing approaches often rely on high-dimensional pixel spaces or generic visual embeddings that retain many factors irrelevant to control, limiting efficiency and generalization across tasks. To this end, we study how agents can learn world models with representations that are *task-specific*, *minimal*, and *sufficient* for decision making. We achieve this via a closed-loop synergy between the *agent* and the *world model*, in which structured world-model learning distills task-sufficient representations from informative interaction data. On the agent side, agents perform *active probing* of the environment to collect informative trajectories that expose task-relevant latent factors, guided by an adaptive curriculum. On the world-model side, we learn *structured representations* over observations to distill compact, task-sufficient latent states from the collected interaction data. This synergy enables the recovery of task-sufficient latent representations that capture all control-relevant factors. Leveraging these representations, the resulting policies achieve sample-efficient generalization in novel settings, including generalization across skills, object–skill compositions, and previously unseen tasks on continuous control and robotic manipulation benchmarks. Project website is here.

1. Introduction

World models (Ha & Schmidhuber, 2018) are generative or predictive models that capture environment observation functions, dynamics, and rewards; in model-based RL (MBRL), it benefits planning, policy improvement, and simulated rollouts to reduce sample complexity (Sutton, 1991). One way of learning the world model is to compress raw observations into meaningful latent states that support accurate prediction and control, facilitating reuse across tasks and improving generalization, e.g., Dreamer-series (Hafner et al., 2020; 2021; 2025), Efficient-Zero (Schrittwieser et al., 2020; Ye et al., 2021), and TD-MPC (Hansen et al., 2022; 2024). Recent work also leverages pre-trained foundation models as strong perceptual encoders: using embeddings as the observation space, and the agent then learns dynamics on top of these embeddings via self-predictive manners (Zhou et al., 2025; Baldassarre et al., 2025; Kapoor et al., 2025; Wang et al., 2025; Assran et al., 2025).

These models often excel at learning visual dynamics and supporting downstream control. Yet their internal representations frequently entangle perceptual factors unrelated to control, which can yield brittle policies in complex or changing environments (Wang et al., 2022a; Liu et al., 2023; Vafa et al., 2025). By contrast, humans typically do not plan using pixel-level predictions or by tracking redundant perceptual details; instead, our planning relies on compact task-relevant representations (Mastrogiuseppe & Ostojic, 2018; Ho et al., 2022; Rajalingham et al., 2022; Nayebi et al., 2023). Motivated by this, we argue that learning world models with *task-specific, minimal sufficient* latents, derived from raw observations or foundation-model priors, is essential for policy learning, as such representations preserve exactly the information needed for decision-making.

In pursuit of these minimal and sufficient representations in world models, we draw inspiration from how humans acquire structured knowledge through interaction. A child actively probes the environment, selectively seeking informative experiences and gradually mastering abstract concepts in a structured manner (Schulz et al., 2008; Bonawitz et al., 2011). Similarly, for agent learning with world models, we can decompose the problem into two coupled components: interactive data curation by the **agentic exploration** and a **structured world model** learning framework that distills task-sufficient representations. These two components form

[*]Equal contribution [1]UCSD [2]MBZUAI [3]CMU [4]UBC. Correspondence to: Fan Feng <ffeng1017@gmail.com>.

Proceedings of the 43rd International Conference on Machine Learning, Seoul, South Korea. PMLR 306, 2026. Copyright 2026 by the author(s).

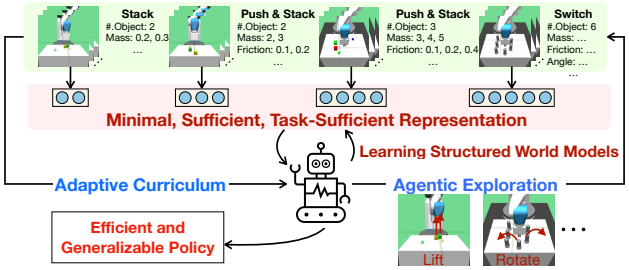

Figure 1. **Overview on** MIST-WM: co-evolve on the agentic exploration and structured world models. The agent conducts active interventions to curate meaningful behavior data to identify the key latent factors in each new environment under an adaptive curriculum. With the curated data, a structured world model with minimal, sufficient, and task-specific representation is learned.

a closed-loop synergy centered on learning task-sufficient representations for world models. Agentic exploration determines *what data are collected*, while structured world-model learning determines *how task-relevant information is distilled* from that data.

We term this framework MIST-WM (Minimal, Sufficient, and Task-specific World Model), which considers the general setting of agents facing a sequence of tasks, and co-evolves agentic exploration with structured world-model learning across these tasks (Fig. 1). The agent learns world models sequentially, using each previously learned model as a prior for the next, yielding a latent space that progressively expands while remaining well-structured. This is achieved through a closed-loop interaction between agentic exploration and world models. Upon encountering a new task, the agent actively designs and executes probing behaviors via self-supervised skills to collect trajectories that maximize expected information gain about task-specific latent factors. The interaction data is then used to learn a structured world model under objectives that enforce minimality and sufficiency, yielding compact and structured representations. Together, these components enable MIST-WM to (i) learn task-specific latent representations that are minimal and sufficient across a sequence of tasks, and (ii) support sample-efficient generalization in novel settings, as policies conditioned on sufficient representations can reuse control-relevant factors and adapt efficiently to novel tasks without irrelevant structure.

Overall, MIST-WM offers an end-to-end recipe for what data to collect, how to learn the world model, and how to generalize across tasks via the reuse of learned representation. We evaluate on locomotion and robotic control benchmarks, in which MIST-WM learns task-specific representations that are both minimal and sufficient, aligning with true system variables. With these compact representations, it achieves sample-efficient generalization in novel settings, at the skill level, in object–skill compositions, and on unseen tasks by composing the previously learned representation.

2. Preliminaries

In this section, we formally define minimal and sufficient task-specific representations and the corresponding structured world models. We consider a general setting where an agent encounters a sequence of tasks whose underlying state factors may vary across tasks, e.g., new objects, dynamics, or reward-relevant variables may be introduced over time.

To capture the essential structures under this setting, we model the environment as a factored partially observable Markov decision process (POMDP) (Boutilier et al., 2000) with an expandable latent state space, allowing new state variables to be introduced as the agent transitions to new tasks. We then define the *Minimal, Sufficient, Task-specific* (MIST) states and outline the computational flow for identifying and using MIST within the world model.

Factored POMDP with Changing Structure and Expandable States. We model the system as a factored POMDP, which can be represented as a tuple $\mathcal{M} = \big(\mathcal{S}, \mathcal{A}, \mathcal{O}, \gamma, \mathcal{G}, \mathbb{P}_s, \mathbb{P}_o, \mathcal{R}, \rho_0\big)$, where $\mathcal{S}$ is the (latent) state space, $\mathcal{A}$ the action space, $\mathcal{O}$ the observation space, $\gamma \in (0,1)$ the discount, and ρ_0 an initial-state distribution. $\mathcal{G}$ is a Dynamic Bayesian Network (DBN) (Murphy et al., 2002) over state factors $\mathbf{s}_t = (\mathbf{s}_t^1, \dots, \mathbf{s}_t^d)$, action $\mathbf{a}_t = (\mathbf{a}_t^1, \dots, \mathbf{a}_t^m)$ and reward r_t. Let $\mathrm{pa}(X)$ denote the set of parents of node X in $\mathcal{G}$. Hence, the state transitions are $\mathbb{P}_s(\mathbf{s}_t \mid \mathbf{s}_{t-1}, \mathbf{a}_{t-1}) = \prod_{i=1}^d \mathbb{P}_s\big(\mathbf{s}_t^i \,|\, \mathrm{pa}(S_t^i)\big)$, where $\mathrm{pa}(S_t^i) \subseteq \{\mathbf{s}_{t-1}^1{:}\mathbf{s}_{t-1}^d,\ \mathbf{a}_{t-1}^1{:}\mathbf{a}_{t-1}^m\}$. The task-specific reward is a function of the parents of R_t: $\mathcal{R}(s_t, a_t) = \mathbb{E}[R_t \mid \mathrm{pa}(R_t)]$, where $\mathrm{pa}(R_t) \subseteq \{\mathbf{s}_t^1{:}\mathbf{s}_t^d,\ \mathbf{a}_t^1{:}\mathbf{a}_t^m\}$. The observation function is modeled as $\mathbb{P}_{\mathbf{o}}(\mathbf{o}_t \mid \mathbf{s}_t) = \prod_{j=1}^p \mathbb{P}_o\big(\mathbf{o}_t^j \,|\, \mathrm{pa}(\mathbf{o}_t^j)\big)$, where $\mathrm{pa}(\mathbf{o}_t^j) \subseteq \{\mathbf{s}_t^1{:}\mathbf{s}_t^d\}$.

Then we consider a sequence of tasks $\{T_i\}_{i=1}^N$, where the latent state space is allowed to grow over time. Specifically, when the agent transitions to a new task, new state variables may be introduced that were absent in previous tasks. Thus, in task T_i, the latent state is $\mathbf{s}_t^i = (\mathbf{s}_t^{i,1}, \dots, \mathbf{s}_t^{i,d_i})$, where $d_1 \le \cdots \le d_N$, allowing the state dimensionality to *expand across tasks*. Each task is equipped with a task-specific DBN $\mathcal{G}^{(i)}$ over $(\mathbf{s}_t^i, \mathbf{a}_t, \mathbf{o}_t, r_t^i)$. The corresponding state transition $\mathbb{P}_s^{(i)}$, observation function $\mathbb{P}_o^{(i)}$, and reward function $\mathcal{R}^{(i)}$ are also task-specific, yielding the task-specific DBNs (Bilmes, 2000). Fig. 2(a) illustrates two tasks with different state–transition ($\mathbf{s}_t \to \mathbf{s}_{t+1}$) and state–reward ($\mathbf{s}_t \to r_t$). In addition, task 2 introduces an additional state factor $\mathbf{s}^{2,3}$.

Definition 1 (MIST indices for task T_i)**.** *Let task T_i have factored state $\mathbf{s}_t^i = (\mathbf{s}_t^{i,1}, \dots, \mathbf{s}_t^{i,d_i})$ and a dynamic Bayesian network $\mathcal{G}^{(i)}$ with parent operator $\mathrm{pa}_{\mathcal{G}^{(i)}}(\cdot)$. Define the current-time MIST indices*

$$I_{i,1}^{(t)} := \big\{k \in [d_i] \mid \mathbf{s}_t^{i,k} \in \mathrm{pa}_{\mathcal{G}^{(i)}}(r_t)\big\},$$

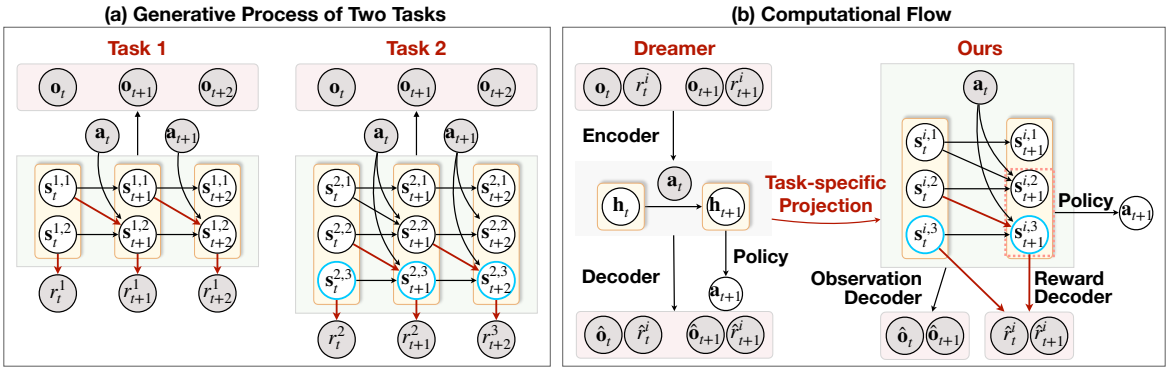

Figure 2. (a) Example DBNs that describe the generative process of two tasks. The grey and white nodes indicate observable and latent variables. The blue nodes are the newly expanded variables for Task 2. Red edges are the links from state variables to rewards. For simplicity, we omit the factorization of the state–observation mapping $\mathbf{s} \to \mathbf{o}$. (b) Computational flow of our proposed framework compared with the Dreamer-based world model.

and their one-step parent indices

$$I_{i,2}^{(t)} := \{k \in [d_i] \mid \exists\, j \in I_{i,1}^{(t)} \text{ such that } \mathbf{s}_{t-1}^{i,k} \in \mathrm{pa}_{\mathcal{G}^{(i)}}(\mathbf{s}_t^{i,j})\}.$$

The MIST index set is $U_i := I_{i,1}^{(t)} \cup I_{i,2}^{(t)}$.

We provide formal definitions of sufficiency and minimality in Appendix B.1. An illustrative example of identifying the minimal sufficient states for each task is shown in Fig. 2(a). The MIST states for task 1 and 2 are $\{\mathbf{s}^{1,1}, \mathbf{s}^{1,2}\}$ and $\{\mathbf{s}^{2,2}, \mathbf{s}^{2,3}\}$, respectively, traced by red edges.

MIST for World Model & Policy Learning. Given the MIST states, we can employ them directly for policy learning. For a concise comparison, Fig. 2(b) contrasts our approach with Dreamer-based methods (Hafner et al., 2021; 2025). While Dreamer learns unstructured latent states, we obtain compact, task-specific representations by projecting Dreamer-style latents through our structured decomposition and masking unrelated components. Consequently, our policy can be produced solely from the MIST states (pink dashed nodes in the right panel). Similarly, reward reconstruction uses only the reward's parent variables (blue nodes), thereby respecting the identified structure.

3. Method

With the formal definition of MIST states in place, we now present the algorithmic framework of learning `MIST-WM` (Fig. 3, Algorithm 1). The framework consists of two *interleaved* stages: *agentic exploration* within the environment and *structured world model learning*. In the remainder of this section, we first describe how the structured world model is learned. We then explain how, for each new task, agentic exploration discovers and collects informative interaction data for learning MIST representations. Finally, we introduce the adaptive curriculum, which facilitates agentic exploration by sequentially selecting tasks and their order.

3.1. Learning Structured World Models

Our structured world model can be built on top of any off-the-shelf world-model backbone by learning a structured latent decomposition over its latent states. In this work, we instantiate our approach using Dreamer-V3 (Hafner et al., 2025) as the base model. For each task T_i, we learn a generative world model with the standard variational objective in Dreamer-V3 (Hafner et al., 2025):

$$\mathcal{L}_{\mathrm{WM}}^{i}(\theta) = \mathbb{E}_{\mathcal{D}}\Bigg[-\sum_{t=0}^{T-1} \log p_\theta(\mathbf{o}_t \mid \mathbf{s}_t^i) - \log p_\theta(r_t^i, \gamma_t^i \mid \mathbf{s}_t^i) + \beta\, \mathrm{KL}\big(q_\theta(\mathbf{s}_t^i \mid \mathbf{o}_t, \mathbf{s}_{t-1}^i, \mathbf{a}_t) \,\|\, p_\theta(\mathbf{s}_t^i \mid \mathbf{s}_{t-1}^i, \mathbf{a}_t)\big) \Bigg], \tag{1}$$

where θ denotes the world model parameters. However, this objective alone generally cannot identify the MIST states, since the learned latent space lacks explicit structure (left of Fig. 2(b)). We therefore incorporate a learnable mask $m^i \in (0,1)^d$ to select the task-specific subspace $\mathcal{S}_i^{\min}$ for task T_i: $m^i \odot \mathbf{s}_t^i \in \mathcal{S}_i^{\min}$, where $\mathbf{s}_t^i \in \mathbb{R}^d$ is the learned latent state from Dreamer. In order to learn this mask, we have **Sufficiency Score** $\mathcal{R}_{\mathrm{suff}}^{(i)}(\theta)$ and the **Minimality Score** $\mathcal{R}_{\min}^{(i)}(\theta)$ as follows.

The sufficiency score uses the masked states to maximize the likelihood of the observed rewards:

$$\mathcal{R}_{\mathrm{suff}}^{(i)} = \mathbb{E}_{\mathcal{D}}\left[\sum_{t=0}^{T-1} \log p_\theta\big(r_t \mid m^i \odot \mathbf{s}_t^i, \mathbf{a}_t\big)\right]. \tag{2}$$

For the minimality score, we encourage the mask to retain only the necessary state dimensions by maximizing the mutual information between the masked states and the task

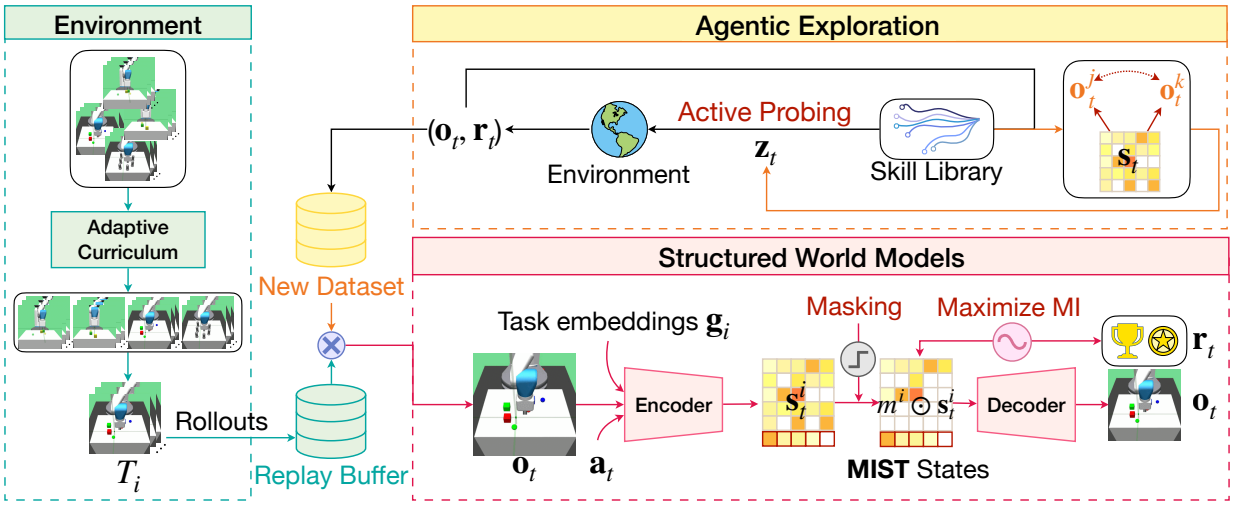

Figure 3. **Method overview.** On the agent side, for each new environment, the agent selects skills from its library to perform *active probing*, collects informative data, under an adaptive curriculum. Conditioned on these informative data, the *structured world model* is learned to distill the MIST states.

descriptor, while penalizing the mask's ℓ_1 norm:

$$\mathcal{R}_{\min}^{(i)} = \mathrm{MI}\big(m^i \odot \mathbf{s}_{1:T}^i, \mathbf{g}^i\big) - \lambda_M \, \|m^i\|_1, \tag{3}$$

where λ_M is a balancing coefficient and $\mathbf{g}_i$ is the auxiliary task-specific information (e.g., task instructions). For the task descriptor, when a simulator-provided task instruction is available, we encode this context using a pretrained RoBERTa (Liu et al., 2019) and use the resulting representation as the task embedding; otherwise, we use rewards only. Hence, in practice, it is either a pretrained task embedding or scalar reward information, depending on the benchmark. At test time, the same form of task information is provided as in training. Note that our method is a practical surrogate for the formal DBN-defined MIST states, aiming to recover a MIST-aligned task-specific subspace rather than exact latent DBN variables.

We use the world model with Dreamer-v3 (Hafner et al., 2025) to obtain the latent states, learn the soft mask m^i via a gating-mask objective adapted from Rajamanoharan et al. (2024), and estimate the mutual information term using MINE (Belghazi et al., 2018). Both approximated objectives are provided in Appendix C.1. When moving to a new task (Fig. 2(a)), the dimensionality of the latent state is allowed to increase every time. Concretely, when transitioning from task T_i to T_{i+1}, we fine-tune the encoder parameters learned for T_i and adapt the final layer to accommodate the additional state dimensions required by T_{i+1}. This preserves the previously learned subspace while expanding the representation for new task-specific factors. Specific network details are in Appendix C.4.

With these structure-learning objectives, we can identify the MIST subspace from the learned latents and restrict downstream control to this subspace; that is, both the policy and value function operate on $\mathcal{S}_i^{\min}$. For task T_i, we optimize the cumulative return $\mathcal{J}_{\mathrm{RL}}^{(i)}(\psi) = \mathbb{E}\left[\sum_{t=0}^{T-1} \gamma^t \, r^i(\mathbf{s}_t^i, \mathbf{a}_t)\right]$, with $\mathbf{a}_t \sim \pi_\psi\big(\cdot \mid m^i \odot \mathbf{s}_t^i\big)$.

3.2. Agentic Exploration

Identifying MIST states requires informative interaction data for each task; without such data, the learned latents $\mathbf{s}^i$ cannot reliably capture the underlying task-relevant factors. Hence, we require informative trajectories that reveal how latent factors influence observations and rewards, rather than the offline datasets passively sampling a limited region of the state space. While on-policy exploration or other active-learning-curated data (Pathak et al., 2017; Sekar et al., 2020; Kauvar et al., 2023) may occasionally provide such coverage, in novel environments, an agent without purposeful exploration will generally struggle to uncover task-relevant structure. Accordingly, upon entering a new environment, we enable such agentic exploration: the agent actively collects data through *active probing*, executing probing skills $\mathbf{z}$ that induce controlled perturbations of the environment to differentiate latent factors.

The probing skills are designed to *maximize* the *information gain* about the world-model parameters θ in a new environment while ensuring broad, task-agnostic state coverage. They are modeled as high-level latent variables $\mathbf{z}$ sampled from a distribution p_η, with actions drawn from a skill-conditioned policy $\pi_\varepsilon(\mathbf{a} \mid \mathbf{s}, \mathbf{z})$. Our objective can be decomposed into two consecutive procedures: (i) building a skill library, and (ii) selecting informative skills to probe the environment, enhancing information gain for world models.

Learning the Probing Skill Library $\mathcal{Z}$. Following the

mutual information skill learning (MISL) framework (Eysenbach et al., 2019; Park et al., 2024; Zheng et al., 2025), we learn the *exploration policy* $\pi_\varepsilon(\mathbf{a} \mid \mathbf{s}, \mathbf{z})$ to maximize state–skill mutual information and action entropy.

We select the prior distribution of skills as a uniform distribution over the d-dimensional unit hypersphere (a uniform von Mises–Fisher distribution (Mardia & Jupp, 2009), $p(\mathbf{z}) = \mathrm{Unif}\left(\mathbb{S}^{d-1}\right)$) and learn the *discriminator* $q_\phi(\mathbf{z} \mid \mathbf{s})$ to make skills identifiable from states. We adopt off-the-shelf MISL algorithms; in particular, DIAYN (Eysenbach et al., 2019) and METRA (Park et al., 2024). Details are given in Appendix C.2.

Specifically, we maximize the lower bound of mutual information with the objectives:

$$\max_{\varepsilon,\eta,\phi} \mathbb{E}\Big[\mathcal{H}\big(\pi_\varepsilon(\cdot \mid \mathbf{s}, \mathbf{z})\big) + \log q_\phi(\mathbf{z} \mid \mathbf{s}) - \log p_\eta(\mathbf{z})\Big] \quad (4)$$

where $\mathcal{H}$ computes the conditional entropy. Empirically, we sample a skill $\mathbf{z} \sim p_\eta$ per k steps, roll out $\pi_\varepsilon(\cdot \mid \mathbf{s}, \mathbf{z})$, treat $\log q_\phi(\mathbf{z} \mid \mathbf{s})$ as an intrinsic reward and maximize policy entropy analytically. To capture temporally extended effects, we replace $\mathbf{s}$ with a segment encoder $\phi_{\text{seg}}(\mathbf{s}_{t+1:t+k}, \mathbf{s}_t)$.

Maximizing the Information Gain. Within the skill library, we select skills that maximize information gain, measured by their ability to facilitate the discovery of latent representations. Let $\mathbf{s}_t^{n_i}$ denote the i-th latent factor at time t, taking values in the space $\mathcal{V}_i$. For two distinct values $v, v' \in \mathcal{V}_i$, under the skill-conditioned exploration policy $\pi_\varepsilon(\cdot \mid \mathbf{s}, \mathbf{z})$, we define the k-step observation segments as

$$\mathbf{o}_{t:t+k}^{(v)} \sim \mathcal{P}\Big(\mathbf{o}_{t:t+k} \;\Big|\; \mathbf{s}_t^{(n_i)} = v,\ \pi_\varepsilon(\cdot \mid \mathbf{z})\Big),$$
$$\mathbf{o}_{t:t+k}^{(v')} \sim \mathcal{P}\Big(\mathbf{o}_{t:t+k} \;\Big|\; \mathbf{s}_t^{(n_i)} = v',\ \pi_\varepsilon(\cdot \mid \mathbf{z})\Big).$$

These rollouts can be generated directly by the agent experimenting in the environment, e.g., lifting two cubes with different weights using different skills. A skill is informative if it induces observation segments whose distributions differ markedly for two distinct latent-factor values v and v'. When $\mathcal{V}_i$ is continuous, v and v' can be understood as the valuations of two independent samples from $\mathcal{V}_i$, chosen such that $v \neq v'$. In particular, when $\mathbf{o}_{t:t+k}^{(v)}$ and $\mathbf{o}_{t:t+k}^{(v')}$ are clearly distinguishable, the resulting contrast reveals the latent factors responsible for the difference. Hence, the information gain can be quantified as the separability of segments.

We then encourage this separability of segments produced from different values of $\mathbf{s}_t^{(n_i)}$ via a distance metric. Specifically, we encode each sequence with $\phi_\xi(\cdot)$. For each anchor $\mathbf{o}_{t:t+k}^{v}$, we choose a positive sample $\mathbf{o}_{t:t+k}^{(v^+)}$ from the same valuation of latent variables (i.e., $\mathbf{s}_t^{(n_i)} = v$ but with another rollout segment), and a set of negatives $\{\mathbf{o}_{t:t+k}^{(v')}\}_{v' \in \mathcal{N}(v)}$. We utilize an InfoNCE loss (Oord et al., 2018):

$$\mathcal{L}_{\text{cl}}^{(n_i)}(\varepsilon, \xi) = \mathbb{E}\Big[-\log \frac{\mathrm{d}(\mathbf{x}_v, \mathbf{x}_{v^+})}{\mathrm{d}(\mathbf{x}_v, \mathbf{x}_{v^+}) + \sum_{v' \in \mathcal{N}(v)} \mathrm{d}(\mathbf{x}_v, \mathbf{x}_{v'})}\Big]. \quad (5)$$

where j^+ denotes the positive index and $\mathcal{N}(j)$ the negative set. $\mathbf{x}$ is the encoded trajectory output under actions $a_{t:t+T-1} \sim \pi_\varepsilon(\cdot \mid z)$, and $\mathrm{d}(u, v) := \exp(\mathrm{cosine}(u, v))$. Hence, the learned skills guide interaction to maximize expected information gain about task-relevant factors, yielding data most useful for world-model learning. Other than functioning as "scoring", this objective also updates the exploration policy π_ε to make the agents grasp the skills that prioritize these behaviors.

Adaptive Curriculum for Exploration. To facilitate the agents to collect informative data, we use an adaptive curriculum that selects and orders environment–task pairs to expose the agent to informative transitions for world-model learning with progressively staging difficulty.

First, each environment provides minimal design scaffolding to ensure that such informative segments can be discovered. For example, to encourage the discovery of object mass, we place two cubes with different weights on the workstation and allow the agent to infer the latent factors through interactions. Details are given in Appendix D.2.

We then optimize the ordering of environment and tasks (a permutation σ over $\{T_i\}_{i=1}^N$). Since each task is instantiated in a specific environment, σ is selected to maximize *data efficiency* for both world-model learning and policy learning. To operationalize it, we minimize world-model learning error and maximizing the cumulative rewards across all environments and tasks:

$$\min_\sigma \sum_{j=1}^{N} \mathcal{L}_{\text{WM}}\big(T_{\sigma(j)} \mid \mathcal{D}_{\sigma(<j)}\big) \;-\; \lambda_R \sum_{j=1}^{N} \mathcal{J}_{\text{RL}}^{(\sigma(j))}(\psi).$$

Specifically, for world-model learning, since the latent dynamics are unknown, following (Sekar et al., 2020), we estimate the error via an ensemble $\{f_\theta^{(m)}\}_{m=1}^M$ and define a disagreement. For downstream task learning, let $p_\theta(r \mid \mathbf{s}, \mathbf{a})$ be the reward head conditioned on the current learned latent states. We use the reward loss to measure it directly. Hence, we have the evaluation proxy:

$$C_T(\mathcal{D}) \;:=\; \mathbb{E}_{(\mathbf{s},\mathbf{a})\sim\mathcal{D}}\Big[d_{\text{var}}\Big(\{f_\theta^{(m)}(\mathbf{s}, \mathbf{a})\}_{m=1}^M\Big) - \log p_\theta(r \mid \mathbf{s}, \mathbf{a})\Big]. \quad (6)$$

where d_{var} is the variance. This induces a natural notion of *task difficulty*. Following Unsupervised Experiment Design (UED) (Dennis et al., 2020; Rigter et al., 2024), we first explore all environments with the policy π_ε and then have a buffer of per-task error scores $C_T(\mathcal{D})$. Each time, we

select the next environment to reduce the worst-case error in learning.

Concretely, we first explore all environments with the policy π_ε and maintain a per-task error buffer $C_T(\mathcal{D})$. At each step, we choose the hardest environment, that is, the one with the largest current error, and collect additional data there: $T^\star = \arg\max_T \; C_T(\mathcal{D})$. We then select $T^\star$ for learning. By repeating this procedure iteratively, we progressively reduce the maximum error across environments. In effect, this approximates solving a min–max objective, i.e., minimizing the maximum of the total error in the world models.

4. Related Works

Structures in World Model Identifying meaningful structure in model-based reinforcement learning (MBRL) and world models is critical for generalization. Prior work can be broadly grouped into three lines. The first line focuses on compact state abstractions in (PO)MDPs. Representative examples include bisimulation-based methods (Ferns et al., 2004; Castro, 2020; Zhang et al., 2021), which aggregate states that are equivalent in return and transition dynamics under the abstraction. Other model-free approaches instead incorporate contrastive objectives to learn invariant features, as in CURL (Laskin et al., 2020). The second line aims to learn task- or control-aware representations in a model-based manner. Methods such as TIA (Fu et al., 2021) and Denoised MDP (Wang et al., 2022a) learn representations tailored to controllability or task-specific representations, thereby improving planning. The third line recovers structured world models by identifying graph structure in MDPs or POMDPs, i.e., learning factored MDPs (Boutilier et al., 2000) from data. These approaches assume and exploit an underlying causal graph, either over observable states (Pitis et al., 2020; Huang et al., 2021; Wang et al., 2022b; Feng et al., 2022; Ji et al., 2024; Chuck et al., 2025; Cao et al., 2025) or latent states (Liu et al., 2023; Hwang et al., 2024), to support more generalizable decision making. Our work is most closely related to the last two lines but differs from them: rather than learning generic controllable representations or full graph structures, we explicitly target *task-specific minimal sufficient* representations. In particular, we recover a factored structure but focus only on the components causally connected to the task, yielding compact, control-sufficient latents that can be integrated directly into policy learning.

Unsupervised RL aims to acquire meaningful behavior without external rewards, and prior work largely follows two directions. One direction focuses on *intrinsic motivation*, where agents optimize surrogate signals that capture knowledge or competence about the environment. Examples include modeling prediction error as a novelty signal (Burda et al., 2019), using curiosity-based measures (Pathak et al., 2017; Kauvar et al., 2023), estimating disagreement among ensemble models (Sekar et al., 2020), and increasing empowerment or controllability across environments (Eysenbach et al., 2019; Tiomkin et al., 2024). The other direction emphasizes *unsupervised skill discovery*, where those methods maximize the mutual information between latent skills and states to learn diverse, meaningful behaviors (Eysenbach et al., 2019; Park et al., 2024; Hu et al., 2024; Zheng et al., 2025). Our work is most closely aligned with the latter: the *active intervention* component of `MIST-WM` learns latent skills specifically to probe the environment and expose task-relevant latent factors, thereby enabling the identification of minimal, sufficient representations for downstream control. For curriculum learning, we draw inspiration from unsupervised environment design (UED) (Dennis et al., 2020; Rigter et al., 2024), which provides curricula over sets of tasks for either policy learning or world-model learning. The work of Dennis et al. (2020) focuses on designing environments specifically for policy learning, while Rigter et al. (2024) studies reward-free cases. In contrast, our approach considers both settings simultaneously: we leverage the learned world model itself to progressively guide task selection to shape the curriculum.

5. Experiments

We evaluate `MIST-WM` whether it can recover task-sufficient representations, and more importantly, whether these representations translate into improved downstream policy learning, particularly in terms of generalization.

Benchmarks & Baselines. For a comprehensive evaluation, we test `MIST-WM` on DMControl(Cheetah, Walker, Reacher in (Tunyasuvunakool et al., 2020)), RoboSuite (Zhu et al., 2020), and Meta-World (Yu et al., 2020), and compare against baselines spanning the design space: world-model backbones (Dreamer-V3 (Hafner et al., 2025), DINO-WM (Zhou et al., 2025), TD-MPC2 (Hansen et al., 2023)), factorization methods (Factored Dreamer (Liu et al., 2023)), intrinsic-motivation approaches (Curiosity Replay (Kauvar et al., 2023), Plan2Explore (Sekar et al., 2020)), and MISL methods (METRA (Park et al., 2024)).

> **RQ1: Representation Recoverability**: *Does the learned latent space recover minimal and task-sufficient representations that capture the essential factors for control?*

We use a controlled RoboSuite setup ((Zhu et al., 2020), Fig. 4a) where ground-truth states are accessible in simulators, allowing us to directly assess whether the learned representation recovers the underlying latent factors. Specifically, we assess whether `MIST-WM` can recover a minimal, task-sufficient subspace by mapping learned coordinates to ground truth via linear probes and reporting alignment

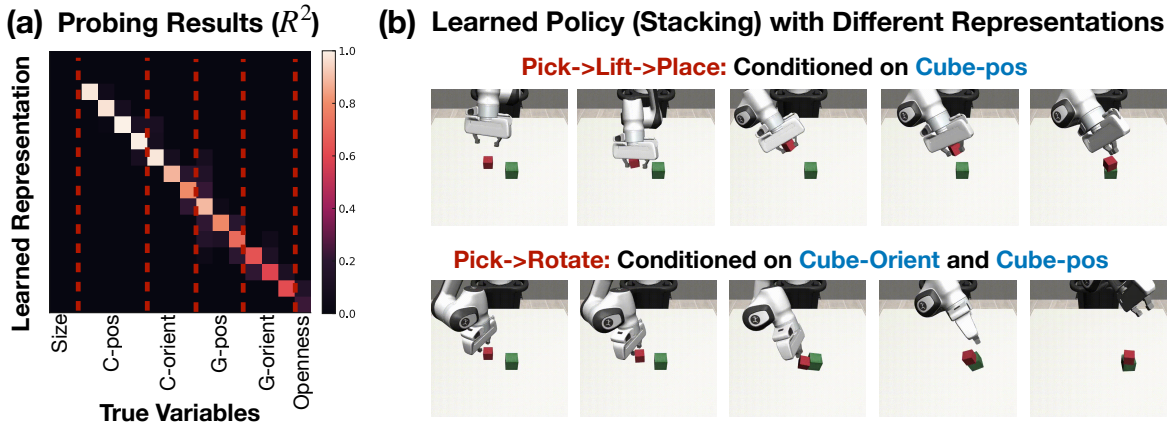

(c) Probing Results Compared with Different Baselines

	Random	METRA	Curiosity Replay	Plan2Explore	DINO-WM	I-Factor	Denoised MDP	MIST-WM
R^2	0.31	0.59	0.44	0.45	0.40	0.48	0.56	**0.78**

Figure 4. Results on Robosuite Stacking environment. (a) The probing results (R^2) matrix ("C" and "G" mean "cube" and "gripper" respectively), and (b) Different policies conditioned on different learned representation variables. (c) Probing results on Robosuite.

R^2 (coefficient of determination (Wright, 1921)).The procedure for mapping the learned representations to ground-truth variables is detailed in Appendix C.7. We also compare the learned representations with ablations and baselines through analyses along two axes: *(i) Data collection:* Random (matched budget), MISL-only (METRA (Park et al., 2024)), and intrinsic-reward methods (Curiosity Replay (Kauvar et al., 2023) and Plan2Explore (Sekar et al., 2020)). *(ii) World model:* using foundation-model (DINO-WM (Zhou et al., 2025)) and factorized models (I-Factor (Liu et al., 2023), Denoised MDP (Wang et al., 2022a)).

Take-Away 1: MIST-WM can recover task-relevant representations. As shown in Fig. 4(a), we obtain near one-to-one alignment for task-relevant factors, including cube position/orientation and gripper position/orientation. However, the static or non-intervenable variables (e.g., object size) are not identified. Likewise, very fine-grained cues (i.e., the gripper open/close states) are not identified: though such signals exist in the data, they are hard to capture with contrastive pairs. In general, MIST-WM identifies a compact subspace that retains what matters for the task and discards others. Fig. 4(c) shows the average R^2 (diag) and Appendix Table A9 gives the full results and Appendix C.7 gives the calculation details. We find that learned MIST-WM attains the highest alignment. Within different data curation methods, aside from ours, METRA yields the best alignment, while intrinsic-reward methods are comparable. For world models, structural representation learning (I-Factor and Denoised MDP) outperforms DINO-WM on average, suggesting the effectiveness of learning disentangled representations of these two.

Take-Away 2: Different learned state representations induce qualitatively different policy behaviors. In RoboSuite Stacking (Fig. 4(c)), conditioning the policy on position features alone yields an optimal pick–lift–place sequence. In contrast, conditioning on both orientation and position enables a shortcut: when the objects are close, the agent can directly rotate one object onto the other. This indicates that an aligned latent space provides more controllable and interpretable behaviors.

> **RQ2: Policy Learning**: *Given a fixed task sequence, do policies trained on MIST states achieve strong sample efficiency relative to baseline world models?*

We consider evaluating the single task policy learning (*no curriculum, only with MIST states learning and active probing skills*) on benchmarks, including robotic control (Meta-World (Yu et al., 2020)) and locomotion tasks from DMControl (Tunyasuvunakool et al., 2020). We compare against DINO-WM (Zhou et al., 2024), I-Factor (a Dreamer-based factored model; labeled *Factored Dreamer*) (Liu et al., 2023), Dreamer-V3 (Hafner et al., 2025), and TD-MPC2 (Hansen et al., 2024). Regarding policy learning, for DMControl and Franka-kitchen, all methods use Proximal Policy Optimization (PPO, (Schulman et al., 2017)), whereas for Meta-World and RoboSuite, they use Soft Actor-Critic (SAC, (Haarnoja et al., 2018)). Results are in Fig. 5 with full results in Appendix Fig. A3, Table A10-A11. Computational cost analysis is given in Appendix D.4.

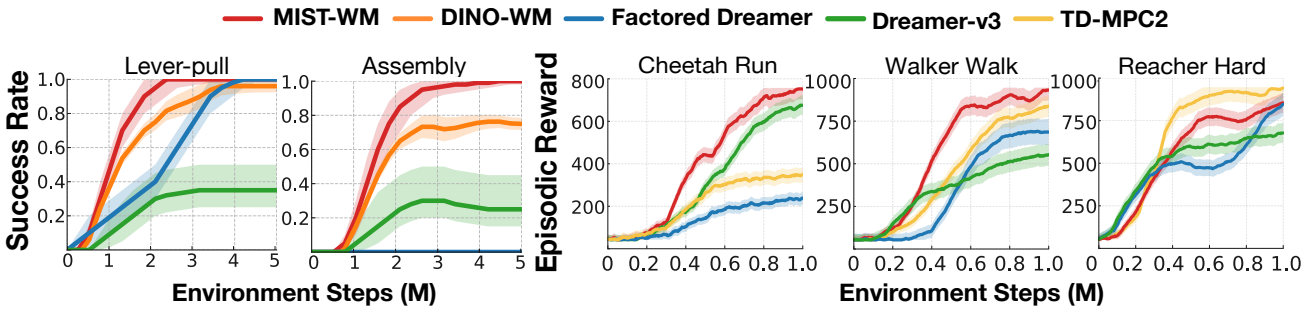

Figure 5. Results (across 5 seeds) on single-task learning, including **robotic manipulation** tasks (Meta World) and **locomotion** (DMControl). Shaded areas indicate the standard errors.

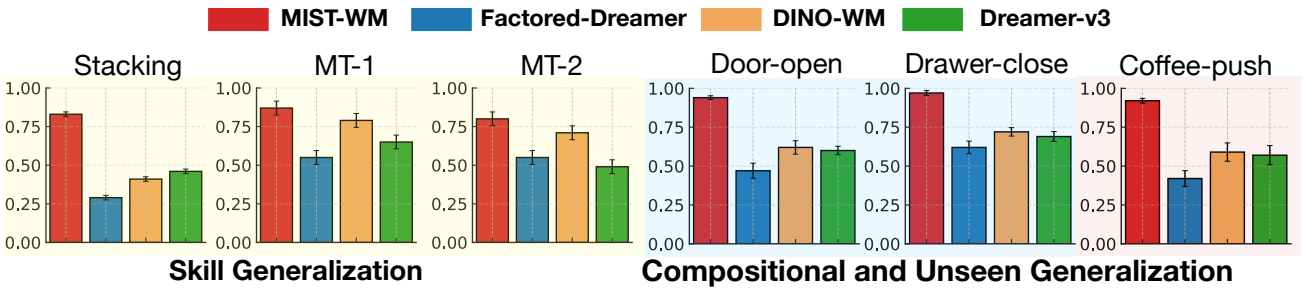

Figure 6. Success rate (across 5 seeds) on skill and compositional generalization, including tasks in Stacking (Robosuite), MT-1 & 2 (kitchen), and Door-open, Door-close, Coffee-push (Meta-World). Error bars indicate the standard errors.

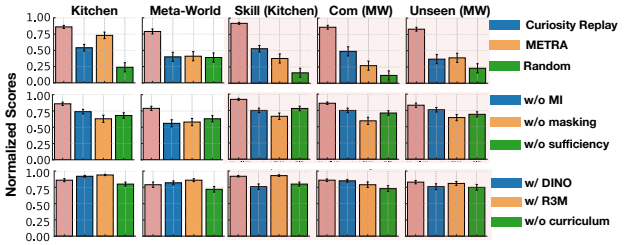

Figure 7. **Ablation studies**. We consider studies on exploration policy (Row 1); World model terms (Row 2); and Backbones and curriculum (Row 3). Pink bars are original `MIST-WM` and error bars indicate the standard errors.

Take-Away 3: `MIST-WM` consistently improves data efficiency and policy learning performances across most tasks, except for Reacher-Hard. On Meta-World, DINO-WM is typically the second-best, while Factored Dreamer and Dreamer-V3 often lag behind DINO-WM. On locomotion, `MIST-WM` outperforms TD-MPC2 on Cheetah and Walker but underperforms on Reacher-Hard, while still exceeding Dreamer-based baselines. We attribute this to differing objectives: TD-MPC optimize a model-free control objective, whereas `MIST-WM` builds on Dreamer objectives.

RQ3: Sample-Efficiency and Generalization: *Do the learned task-sufficient representations transfer beyond the training tasks, enabling systematic generalization in policy learning?*

We evaluate `MIST-WM` on three types of generalization using the learned MIST representations. Summary results are in Fig. 6 and full results are in Fig. A4.

Take-Away 4: The learned MIST representations consistently improve skill, compositional, and unseen-task generalization. *(i) Skill generalization.* Can the learned MIST states facilitate better skill-level generalization? We study this in RoboSuite (Zhu et al., 2020) and Franka-Kitchen (Gupta et al., 2019), where source tasks are learned and then transferred to target tasks that require composing multiple the learned representations. Results show that `MIST-WM` achieves large improvements on both source and target tasks, with especially pronounced gains in RoboSuite target tasks and harder Kitchen tasks (e.g., Kitchen-light). This suggests that the learned representation help scale to complex, long-horizon behaviors. *(ii) Compositional generalization.* Here we combine learned "objects" and "skills" to create novel tasks. In Meta-World (Yu et al., 2020), we train on (door-unlock, drawer-open, faucet-close, handle-pull) and evaluate on (door-open, drawer-close). `MIST-WM`

outperforms all baselines on both base and target tasks, with especially strong gains on the door-open target. *(iii) Unseen-task generalization.* Finally, in Meta-World, we test on coffee-push, a task where neither "coffee" nor "push" appeared during training. MIST-WM generalizes well, indicating that the learned latent representations capture transferable structure that extends to previously unseen factors. We learn an expandable state space that supports new tasks. When a task involves new combinations of skills or objects, the agent can initialize from previously learned states and learn the corresponding policy with fewer samples.

> Ablation Studies To evaluate each component of MIST-WM, we conduct ablations along three axes: *(i) Different policy* for data curation: *Random*, *Intrinsic motivation* (Curiosity Replay (Kauvar et al., 2023)), and *MISL* (METRA); *(ii) World Model terms*: removing the MI term in the *minimality* score, removing *masking* in the minimality score, and removing the *sufficiency* term; and *(iii) Backbone and curriculum*: replacing the Dreamer-v3 encoder with *DINO-WM* or *R3M*, and training w.r.t. a *no-curriculum* variant (i.e., random order). We report both single-task learning and cross-environment generalization (Fig. 7, full results are in Appendix Fig. A6). All scores are normalized to an *Oracle* that directly receives ground-truth states in each environment.

Take-Aways for Ablations: The default MIST-WM achieves the best overall. In generalization settings (pink panels), performance approaches the Oracle (often ≈ 0.9), and exceeds single-task learning, indicating that the *learned representations transfer across tasks*. For case (i), METRA is typically second-best, while Random is consistently worst. On generalization tasks, Curiosity Replay sometimes surpasses METRA, consistent with its broader, task-agnostic coverage, improving transfer. For case (ii), Removing MI, masking, or sufficiency uniformly degrades performance. The effects are similar in single-task settings; in generalization, masking has the largest impact, suggesting that enforcing compactness improves transfer. For case (iii), using DINO-WM (Zhou et al., 2024) or R3M (Nair et al., 2023) features can help on some tasks, but is not consistently superior. Removing the curriculum causes larger drops in generalization than in single-task learning, reflecting the curriculum's role in generalization across tasks. Results indicate that synergy between agentic exploration (probing skills) and structured models is crucial, as the absence of either component leads to degraded information acquisition and suboptimal learning dynamics.

6. Conclusion

We study how agents can learn world models whose latent spaces provide task-sufficient representations. Our goal is to distill compact latent representations directly from pixels, focusing the agent on task-relevant factors. To this end, we synergize agentic exploration with structured world-model learning in a closed-loop manner: agentic exploration curates informative interaction data through active probing under an adaptive curriculum, while structure-aware learning objectives leverage these data to distill minimal and sufficient representations in the world model, which in turn guide subsequent exploration. This provides a principled way to learning meaningful representations for world models, enabling efficient and generalizable policy learning.

Impact Statement

This paper presents work whose goal is to advance the field of Machine Learning. There are many potential societal consequences of our work, none of which we feel must be specifically highlighted here.

Acknowledgment

We would like to acknowledge the support from NSF Award No. 2229881, AI Institute for Societal Decision Making (AI-SDM), the National Institutes of Health (NIH) under Contract R01HL159805, and grants from Quris AI, Florin Court Capital, MBZUAI-WIS Joint Program, and the Al Deira Causal Education project.

References

Mido Assran, Adrien Bardes, David Fan, Quentin Garrido, Russell Howes, Matthew Muckley, Ammar Rizvi, Claire Roberts, Koustuv Sinha, Artem Zholus, et al. V-jepa 2: Self-supervised video models enable understanding, prediction and planning. *arXiv preprint arXiv:2506.09985*, 2025.

Federico Baldassarre, Marc Szafraniec, Basile Terver, Vasil Khalidov, Francisco Massa, Yann LeCun, Patrick Labatut, Maximilian Seitzer, and Piotr Bojanowski. Back to the features: Dino as a foundation for video world models. *arXiv preprint arXiv:2507.19468*, 2025.

Philip Ball, Jack Parker-Holder, Aldo Pacchiano, Krzysztof Choromanski, and Stephen Roberts. Ready policy one: World building through active learning. In *International Conference on Machine Learning*, pp. 591–601. PMLR, 2020.

Mohamed Ishmael Belghazi, Aristide Baratin, Sai Rajeshwar, Sherjil Ozair, Yoshua Bengio, Aaron Courville, and Devon Hjelm. Mutual information neural estimation. In *International conference on machine learning*, pp. 531–540. PMLR, 2018.

Jeff A Bilmes. Dynamic bayesian multinets. In *Proceedings of the Sixteenth conference on Uncertainty in artificial intelligence*, pp. 38–45, 2000.

Elizabeth Bonawitz, Patrick Shafto, Hyowon Gweon, Noah D Goodman, Elizabeth Spelke, and Laura Schulz. The double-edged sword of pedagogy: Instruction limits spontaneous exploration and discovery. *Cognition*, 120 (3):322–330, 2011.

Craig Boutilier, Richard Dearden, and Moisés Goldszmidt. Stochastic dynamic programming with factored representations. *Artificial intelligence*, 121(1-2):49–107, 2000.

Yuri Burda, Harrison Edwards, Amos Storkey, and Oleg Klimov. Exploration by random network distillation. In *International Conference on Learning Representations*, 2019. URL https://openreview.net/forum?id=H1lJJnR5Ym.

Hongye Cao, Fan Feng, Meng Fang, Shaokang Dong, Tianpei Yang, Jing Huo, and Yang Gao. Towards empowerment gain through causal structure learning in model-based rl. *arXiv preprint arXiv:2502.10077*, 2025.

Pablo Samuel Castro. Scalable methods for computing state similarity in deterministic markov decision processes. In *Proceedings of the AAAI Conference on Artificial Intelligence*, volume 34, pp. 10069–10076, 2020.

Zixuan Chen, Ze Ji, Jing Huo, and Yang Gao. Scar: Refining skill chaining for long-horizon robotic manipulation via dual regularization. *Advances in Neural Information Processing Systems*, 37:111679–111714, 2024.

Xiaowei Chi, Peidong Jia, Chun-Kai Fan, Xiaozhu Ju, Weishi Mi, Kevin Zhang, Zhiyuan Qin, Wanxin Tian, Kuangzhi Ge, Hao Li, et al. Wow: Towards a world omniscient world model through embodied interaction. *arXiv preprint arXiv:2509.22642*, 2025.

Caleb Chuck, Fan Feng, Carl Qi, Chang Shi, Siddhant Agarwal, Amy Zhang, and Scott Niekum. Null counterfactual factor interactions for goal-conditioned reinforcement learning. *arXiv preprint arXiv:2505.03172*, 2025.

Michael Dennis, Natasha Jaques, Eugene Vinitsky, Alexandre Bayen, Stuart Russell, Andrew Critch, and Sergey Levine. Emergent complexity and zero-shot transfer via unsupervised environment design. *Advances in neural information processing systems*, 33:13049–13061, 2020.

Benjamin Eysenbach, Abhishek Gupta, Julian Ibarz, and Sergey Levine. Diversity is all you need: Learning skills without a reward function. In *International Conference on Learning Representations*, 2019. URL https://openreview.net/forum?id=SJx63jRqFm.

Fan Feng, Biwei Huang, Kun Zhang, and Sara Magliacane. Factored adaptation for non-stationary reinforcement learning. *Advances in Neural Information Processing Systems*, 35:31957–31971, 2022.

Norm Ferns, Prakash Panangaden, and Doina Precup. Metrics for finite markov decision processes. In *UAI*, volume 4, pp. 162–169, 2004.

Xiang Fu, Ge Yang, Pulkit Agrawal, and Tommi Jaakkola. Learning task informed abstractions. In *International Conference on Machine Learning*, pp. 3480–3491. PMLR, 2021.

Yanjiang Guo, Lucy Xiaoyang Shi, Jianyu Chen, and Chelsea Finn. Ctrl-world: A controllable generative world model for robot manipulation, 2025. URL https://arxiv.org/abs/2510.10125.

Abhishek Gupta, Vikash Kumar, Corey Lynch, Sergey Levine, and Karol Hausman. Relay policy learning: Solving long-horizon tasks via imitation and reinforcement learning. *arXiv preprint arXiv:1910.11956*, 2019.

David Ha and Jürgen Schmidhuber. World models. *arXiv preprint arXiv:1803.10122*, 2(3), 2018.

Tuomas Haarnoja, Aurick Zhou, Pieter Abbeel, and Sergey Levine. Soft actor-critic: Off-policy maximum entropy deep reinforcement learning with a stochastic actor. In *International conference on machine learning*, pp. 1861–1870. Pmlr, 2018.

Danijar Hafner, Timothy Lillicrap, Jimmy Ba, and Mohammad Norouzi. Dream to control: Learning behaviors by latent imagination. In *International Conference on Learning Representations*, 2020. URL https://openreview.net/forum?id=S1lOTC4tDS.

Danijar Hafner, Timothy P Lillicrap, Mohammad Norouzi, and Jimmy Ba. Mastering atari with discrete world models. In *International Conference on Learning Representations*, 2021. URL https://openreview.net/forum?id=0oabwyZbOu.

Danijar Hafner, Jurgis Pasukonis, Jimmy Ba, and Timothy Lillicrap. Mastering diverse control tasks through world models. *Nature*, pp. 1–7, 2025.

N Hansen, X Wang, and H Su. Temporal difference learning for model predictive control. In *International Conference on Machine Learning, PMLR*, 2022.

Nicklas Hansen, Hao Su, and Xiaolong Wang. Td-mpc2: Scalable, robust world models for continuous control. *arXiv preprint arXiv:2310.16828*, 2023.

Nicklas Hansen, Hao Su, and Xiaolong Wang. TD-MPC2: Scalable, robust world models for continuous control. In *The Twelfth International Conference on Learning Representations*, 2024. URL https://openreview.net/forum?id=Oxh5CstDJU.

Mark K Ho, David Abel, Carlos G Correa, Michael L Littman, Jonathan D Cohen, and Thomas L Griffiths. People construct simplified mental representations to plan. *Nature*, 606(7912):129–136, 2022.

Jiaheng Hu, Zizhao Wang, Peter Stone, and Roberto Martín-Martín. Disentangled unsupervised skill discovery for efficient hierarchical reinforcement learning. *Advances in Neural Information Processing Systems*, 37:76529–76552, 2024.

Biwei Huang, Fan Feng, Chaochao Lu, Sara Magliacane, and Kun Zhang. Adarl: What, where, and how to adapt in transfer reinforcement learning. *arXiv preprint arXiv:2107.02729*, 2021.

Inwoo Hwang, Yunhyeok Kwak, Suhyung Choi, Byoung-Tak Zhang, and Sanghack Lee. Fine-grained causal dynamics learning with quantization for improving robustness in reinforcement learning. *arXiv preprint arXiv:2406.03234*, 2024.

Tianying Ji, Yongyuan Liang, Yan Zeng, Yu Luo, Guowei Xu, Jiawei Guo, Ruijie Zheng, Furong Huang, Fuchun Sun, and Huazhe Xu. Ace: off-policy actor-critic with causality-aware entropy regularization. In *Proceedings of the 41st International Conference on Machine Learning*, pp. 21620–21647, 2024.

Parv Kapoor, Abigail Hammer, Ashish Kapoor, Karen Leung, and Eunsuk Kang. Pretrained embeddings as a behavior specification mechanism. *arXiv preprint arXiv:2503.02012*, 2025.

Isaac Kauvar, Chris Doyle, Linqi Zhou, and Nick Haber. Curious replay for model-based adaptation. In *International Conference on Machine Learning*, pp. 16018–16048. PMLR, 2023.

Michael Laskin, Aravind Srinivas, and Pieter Abbeel. Curl: Contrastive unsupervised representations for reinforcement learning. In *International conference on machine learning*, pp. 5639–5650. PMLR, 2020.

Yinhan Liu, Myle Ott, Naman Goyal, Jingfei Du, Mandar Joshi, Danqi Chen, Omer Levy, Mike Lewis, Luke Zettlemoyer, and Veselin Stoyanov. Roberta: A robustly optimized bert pretraining approach. *arXiv preprint arXiv:1907.11692*, 2019.

Yuren Liu, Biwei Huang, Zhengmao Zhu, Honglong Tian, Mingming Gong, Yang Yu, and Kun Zhang. Learning world models with identifiable factorization. *Advances in Neural Information Processing Systems*, 36:31831–31864, 2023.

Zichen Liu, Guoji Fu, Chao Du, Wee Sun Lee, and Min Lin. Continual reinforcement learning by planning with online world models. *arXiv preprint arXiv:2507.09177*, 2025.

Kanti V Mardia and Peter E Jupp. *Directional statistics*. John Wiley & Sons, 2009.

Francesca Mastrogiuseppe and Srdjan Ostojic. Linking connectivity, dynamics, and computations in low-rank recurrent neural networks. *Neuron*, 99(3):609–623, 2018.

Russell Mendonca, Oleh Rybkin, Kostas Daniilidis, Danijar Hafner, and Deepak Pathak. Discovering and achieving goals via world models. *Advances in Neural Information Processing Systems*, 34:24379–24391, 2021.

Kevin P Murphy et al. Dynamic bayesian networks. *Probabilistic Graphical Models, M. Jordan*, 7:431, 2002.

Suraj Nair, Aravind Rajeswaran, Vikash Kumar, Chelsea Finn, and Abhinav Gupta. R3m: A universal visual representation for robot manipulation. In *Conference on Robot Learning*, pp. 892–909. PMLR, 2023.

Aran Nayebi, Rishi Rajalingham, Mehrdad Jazayeri, and Guangyu Robert Yang. Neural foundations of mental simulation: Future prediction of latent representations on dynamic scenes. *Advances in Neural Information Processing Systems*, 36:70548–70561, 2023.

Aaron van den Oord, Yazhe Li, and Oriol Vinyals. Representation learning with contrastive predictive coding. *arXiv preprint arXiv:1807.03748*, 2018.

Seohong Park, Oleh Rybkin, and Sergey Levine. METRA: Scalable unsupervised RL with metric-aware abstraction. In *The Twelfth International Conference on Learning Representations*, 2024. URL https://openreview.net/forum?id=c5pwL0Soay.

Deepak Pathak, Pulkit Agrawal, Alexei A Efros, and Trevor Darrell. Curiosity-driven exploration by self-supervised prediction. In *International conference on machine learning*, pp. 2778–2787. PMLR, 2017.

Silviu Pitis, Elliot Creager, and Animesh Garg. Counterfactual data augmentation using locally factored dynamics. *Advances in Neural Information Processing Systems*, 33: 3976–3990, 2020.

Rishi Rajalingham, Aida Piccato, and Mehrdad Jazayeri. Recurrent neural networks with explicit representation of dynamic latent variables can mimic behavioral patterns in a physical inference task. *Nature Communications*, 13 (1):5865, 2022.

Senthooran Rajamanoharan, Arthur Conmy, Lewis Smith, Tom Lieberum, Vikrant Varma, János Kramár, Rohin Shah, and Neel Nanda. Improving dictionary learning with gated sparse autoencoders. *arXiv preprint arXiv:2404.16014*, 2024.

Marc Rigter, Minqi Jiang, and Ingmar Posner. Reward-free curricula for training robust world models. In *The Twelfth International Conference on Learning Representations*, 2024. URL https://openreview.net/forum?id=eCGpNGDeNu.

Julian Schrittwieser, Ioannis Antonoglou, Thomas Hubert, Karen Simonyan, Laurent Sifre, Simon Schmitt, Arthur Guez, Edward Lockhart, Demis Hassabis, Thore Graepel, et al. Mastering atari, go, chess and shogi by planning with a learned model. *Nature*, 588(7839):604–609, 2020.

John Schulman, Filip Wolski, Prafulla Dhariwal, Alec Radford, and Oleg Klimov. Proximal policy optimization algorithms. *arXiv preprint arXiv:1707.06347*, 2017.

Laura E Schulz, Holly R Standing, and Elizabeth B Bonawitz. Word, thought, and deed: the role of object categories in children's inductive inferences and exploratory play. *Developmental Psychology*, 44(5):1266, 2008.

Ramanan Sekar, Oleh Rybkin, Kostas Daniilidis, Pieter Abbeel, Danijar Hafner, and Deepak Pathak. Planning to explore via self-supervised world models. In *International conference on machine learning*, pp. 8583–8592. PMLR, 2020.

Richard S Sutton. Dyna, an integrated architecture for learning, planning, and reacting. *ACM Sigart Bulletin*, 2(4): 160–163, 1991.

Stas Tiomkin, Ilya Nemenman, Daniel Polani, and Naftali Tishby. Intrinsic motivation in dynamical control systems. *PRX Life*, 2(3):033009, 2024.

Saran Tunyasuvunakool, Alistair Muldal, Yotam Doron, Siqi Liu, Steven Bohez, Josh Merel, Tom Erez, Timothy Lillicrap, Nicolas Heess, and Yuval Tassa. dm_control: Software and tasks for continuous control. *Software Impacts*, 6:100022, 2020.

Keyon Vafa, Peter G Chang, Ashesh Rambachan, and Sendhil Mullainathan. What has a foundation model found? using inductive bias to probe for world models. *arXiv preprint arXiv:2507.06952*, 2025.

Team Wan. Wan: Open and advanced large-scale video generative models. *arXiv preprint arXiv:2503.20314*, 2025.

Tongzhou Wang, Simon Du, Antonio Torralba, Phillip Isola, Amy Zhang, and Yuandong Tian. Denoised mdps: Learning world models better than the world itself. In *International Conference on Machine Learning*, pp. 22591–22612. PMLR, 2022a.

Xinyue Wang and Biwei Huang. Modeling unseen environments with language-guided composable causal components in reinforcement learning. *arXiv preprint arXiv:2505.08361*, 2025.

Yucen Wang, Rui Yu, Shenghua Wan, Le Gan, and De-Chuan Zhan. Founder: Grounding foundation models in world models for open-ended embodied decision making. In *Forty-second International Conference on Machine Learning*, 2025.

Zizhao Wang, Xuesu Xiao, Zifan Xu, Yuke Zhu, and Peter Stone. Causal dynamics learning for task-independent state abstraction. *arXiv preprint arXiv:2206.13452*, 2022b.

Sewall Wright. Correlation and causation. *Journal of agricultural research*, 20(7):557, 1921.

Weirui Ye, Shaohuai Liu, Thanard Kurutach, Pieter Abbeel, and Yang Gao. Mastering atari games with limited data. *Advances in neural information processing systems*, 34: 25476–25488, 2021.

Tianhe Yu, Deirdre Quillen, Zhanpeng He, Ryan Julian, Karol Hausman, Chelsea Finn, and Sergey Levine. Meta-world: A benchmark and evaluation for multi-task and meta reinforcement learning. In *Conference on robot learning*, pp. 1094–1100. PMLR, 2020.

Amy Zhang, Rowan Thomas McAllister, Roberto Calandra, Yarin Gal, and Sergey Levine. Learning invariant representations for reinforcement learning without reconstruction. In *International Conference on Learning Representations*, 2021. URL https://openreview.net/forum?id=-2FCwDKRREu.

Chongyi Zheng, Jens Tuyls, Joanne Peng, and Benjamin Eysenbach. Can a MISL fly? analysis and ingredients for mutual information skill learning. In *The Thirteenth International Conference on Learning Representations*, 2025. URL https://openreview.net/forum?id=xoIeVdFO7U.

Gaoyue Zhou, Hengkai Pan, Yann LeCun, and Lerrel Pinto. Dino-wm: World models on pre-trained visual features enable zero-shot planning. *arXiv preprint arXiv:2411.04983*, 2024.

Gaoyue Zhou, Hengkai Pan, Yann LeCun, and Lerrel Pinto. DINO-WM: World models on pre-trained visual features enable zero-shot planning. In *Forty-second International Conference on Machine Learning*, 2025. URL https://openreview.net/forum?id=D5RNACOZEI.

Yuke Zhu, Josiah Wong, Ajay Mandlekar, Roberto Martín-Martín, Abhishek Joshi, Soroush Nasiriany, and Yifeng Zhu. robosuite: A modular simulation framework and benchmark for robot learning. *arXiv preprint arXiv:2009.12293*, 2020.

Appendix

A. Limitations and Future Works

Several limitations remain. Most notably, our experiments are confined to simulated domains; extending the framework to real-world systems, such as physical robotic platforms, is an important direction for future work. Although our methodology is model-agnostic, scaling it to more expressive and scalable world-model architectures, such as diffusion-based world models (Wan, 2025; Chi et al., 2025; Guo et al., 2025) will be left for future works.

B. Notations and Concepts

B.1. Definitions of Minimality and Sufficiency

Definition 2 (Sufficiency)**.** *The index set U_i is* sufficient *for T_i if*

$$r_t^i \perp\!\!\!\perp (\mathbf{s}_{t-1}^i, \mathbf{s}_t^i) \setminus \left(\mathbf{s}_{t-1}^i|_{I_{i,2}^{(t)}}, \mathbf{s}_t^i|_{I_{i,1}^{(t)}}\right) \mid \left(\mathbf{a}_t, \mathbf{s}_{t-1}^i|_{I_{i,2}^{(t)}}, \mathbf{s}_t^i|_{I_{i,1}^{(t)}}\right). \tag{A1}$$

Equivalently, given $\mathbf{a}_t$, the reward depends on the state only through the current MIST states and their one-step parents.

Definition 3 (Minimality)**.** *A sufficient index set U_i is* minimal *if there exist no strict subsets $J^{(t)} \subsetneq I_{i,1}^{(t)}$ and $J^{(t-1)} \subsetneq I_{i,2}^{(t)}$ such that*

$$r_t^i \perp\!\!\!\perp (\mathbf{s}_{t-1}^i, \mathbf{s}_t^i) \setminus \left(\mathbf{s}_{t-1}^i|_{J^{(t-1)}}, \mathbf{s}_t^i|_{J^{(t)}}\right) \mid \left(\mathbf{a}_t, \mathbf{s}_{t-1}^i|_{J^{(t-1)}}, \mathbf{s}_t^i|_{J^{(t)}}\right). \tag{A2}$$

Equivalently, removing any variable from U_i destroys sufficiency.

B.2. Notations

Table A1 collects the notations used in the theorem proofs for clarity and consistency.

B.3. Concepts

Here we explain a few key concepts used in our framework as a complement of the main paper.

Unstructured latent states We instantiate the world model with a recurrent state-space model (RSSM) as in Dreamer-v3, which produces latent states $\mathbf{s}_t \in \mathbb{R}^d$ from observations $\mathbf{o}_t$ and actions $\mathbf{a}_t$ via

$$q_\theta(\mathbf{s}_{t+1} \mid \mathbf{o}_t, \mathbf{s}_t, \mathbf{a}_t), \qquad p_\theta(\mathbf{o}_t \mid \mathbf{s}_t), \quad p_\theta(\mathbf{s}_{t+1} \mid \mathbf{s}_t, \mathbf{a}_t).$$

These latent states are *unstructured* in the sense that no explicit factorization or task-specific subspace is imposed.

Structure learning On top of the unstructured latents, we perform *structure learning* to extract a task-specific subspace. For each task T_i, let $\mathbf{s}_t^i \in \mathbb{R}^d$ denote the corresponding Dreamer latent and $\mathbf{g}^i$ a task descriptor. We learn a mask $m^i \in (0,1)^d$ and a factored generative model over $(\mathbf{s}_t^i, \mathbf{o}_t, r_t^i)$ conditioned on $\mathbf{g}^i$ to optimize Eq. 2-3 to encourage a low-dimensional, task-sufficient subspace.

MIST states For task T_i, the *Minimal, Sufficient, Task-specific (MIST) states* are the masked latents

$$\tilde{\mathbf{s}}_t^i \;=\; m^i \odot \mathbf{s}_t^i \;\in\; \mathcal{S}_i^{\min},$$

where $\mathcal{S}_i^{\min} \subseteq \mathbb{R}^d$ denotes the minimal sufficient subspace recovered by structure learning. Intuitively, MIST states are those coordinates of $\mathbf{s}_t^i$ that are (i) sufficient for predicting rewards r_t^i given $\mathbf{a}_t$, and (ii) cannot be removed without violating sufficiency.

Concretely, the connection between *masked states*, *latent factors*, and the *expandable state space* is as follows. Dreamer provides an unstructured latent vector $\mathbf{s}_t^i \in \mathbb{R}^{d_i}$ for each task T_i, whose coordinates we interpret as latent factors. As we move to new tasks and the environment introduces additional mechanisms, we allow the latent dimensionality d_i to grow

Table A1. List of notations, explanations, and corresponding value ranges.

Variable	Explanation	Support
$\mathcal{S}$	(latent) state space	$\mathcal{S} \subseteq \mathbb{R}^{d_s}$
$\mathcal{A}$	action space	$\mathcal{A} \subseteq \mathbb{R}^{d_a}$
$\mathcal{O}$	observation space	$\mathcal{O} \subseteq \mathbb{R}^{d_o}$
$\mathcal{D}$	dataset / replay buffer distribution	trajectories over $(\mathbf{s}, \mathbf{a}, \mathbf{o}, r)$
$\mathcal{Z}$	skill library (set of learnable skills)	$\mathcal{Z} \subseteq \mathbb{R}^{d_z}$
γ	discount factor	$\gamma \in (0, 1)$
ρ_0	initial-state distribution	$\rho_0 : \mathcal{S} \to [0, 1]$
$\{T_i\}_{i=1}^N$	set of tasks	$i = 1, \ldots, N$
$\mathbf{s}_t^i = (\mathbf{s}_t^{i,1}, \ldots, \mathbf{s}_t^{i,d_i})$	factored (learned) state of task i	d_i state factors
$I_i^{(t)}$	indices of state factors influencing reward r_t	$I_i^{(t)} \subseteq [d_i]$
$I_i^{(t-1)}$	indices of one-step parents of $I_i^{(t)}$	$I_i^{(t-1)} \subseteq [d_i]$
U_i	union of current and one-step parents	$U_i = I_i^{(t)} \cup I_i^{(t-1)}$
$\mathbf{s}_t^i\|_{I_i^{(t)}}$	current-time MIST states	subset of $\mathbf{s}_t^i$
$\mathbf{s}_{t-1}^i\|_{I_i^{(t-1)}}$	one-step parent MIST states	subset of $\mathbf{s}_{t-1}^i$
$\mathbf{g}_i$	task descriptor / embedding for T_i (can be rewards in simple cases)	$\mathbf{g}_i \in \mathbb{R}^{d_g}$
m^i	soft/binary mask selecting task-specific subspace for T_i	$m^i \in (0, 1)^{d_i}$
$\mathcal{S}^{\min}$	minimal sufficient subspace for task T_i	$\mathcal{S}^{\min} \subseteq \mathcal{S}$
T	horizon length	$T \in \mathbb{N}^+$
$\mathbf{z}$	latent skill variable	$\mathbf{z} \in \mathbb{R}^{d_z}$
$\mathcal{N}(v)$	negative sample index set for contrastive learning	$\mathcal{N}(v) \subseteq \{1, \ldots, N\}$
$\mathbf{x}_v, \mathbf{x}_{v^+}, \mathbf{x}_{v'}$	encoded representations of anchor, positive, and negative samples	$\mathbf{x} \in \mathbb{R}^{d_h}$
Function		
$\mathcal{G}$	dynamic Bayesian network (DBN) over $(\mathbf{s}_t, \mathbf{a}_t, r_t)$	graph structure
$\mathcal{G}^{(i)}$	task-specific DBN over $(\mathbf{s}_t^i, \mathbf{a}_t, \mathbf{o}_t, r_t^i)$	graph structure
$\mathbb{P}_s(\mathbf{s}_t \mid \mathbf{s}_{t-1}, \mathbf{a}_{t-1})$	state transition probability	$\mathcal{S} \times \mathcal{A} \to \Delta(\mathcal{S})$
$\mathbb{P}_o(\mathbf{o}_t \mid \mathbf{s}_t)$	observation function	$\mathcal{S} \to \Delta(\mathcal{O})$
$\mathcal{R}(\mathbf{s}_t, \mathbf{a}_t)$	reward function	$\mathcal{S} \times \mathcal{A} \to \mathbb{R}$
$\mathbb{P}_s^{(i)}(\mathbf{s}_t \mid \mathbf{s}_{t-1}, \mathbf{a}_{t-1})$	transition probability of task i	$\mathcal{S} \times \mathcal{A} \to \Delta(\mathcal{S})$
$\mathbb{P}_o^{(i)}(\mathbf{o}_t \mid \mathbf{s}_t)$	observation function of task i	$\mathcal{S} \to \Delta(\mathcal{O})$
$\mathcal{R}^{(i)}(\mathbf{s}_t, \mathbf{a}_t)$	reward function of task i	$\mathcal{S} \times \mathcal{A} \to \mathbb{R}$
$\mathrm{pa}_{\mathcal{G}^{(i)}}(\cdot)$	parent operator in task-specific DBN $\mathcal{G}^{(i)}$	node $\mapsto$ set of parents
$\mathcal{L}_{\text{WM}}^i(\theta)$	task-conditioned world model objective for T_i	variational training loss
$\mathcal{R}_{\text{suff}}^{(i)}(\theta)$	sufficiency score	$\mathbb{E}_{\mathcal{D}}\Big[\sum_{t=0}^{T-1} \log p_\theta\big(r_t \mid m^i \odot \mathbf{s}_t^i, \mathbf{a}_t\big)\Big]$
$\mathcal{R}_{\min}^{(i)}(\theta)$	minimality score for selecting $\mathcal{S}^{\min}$	model-dependent criterion
$p_\theta\big(r_t \mid m^i \odot \mathbf{s}_t^i, \mathbf{a}_t\big)$	conditional reward likelihood (task i)	scalar density
$\mathcal{J}_{\text{RL}}^{(i)}(\psi)$	expected cumulative return objective for task i	$\mathbb{E}\Big[\sum_{t=0}^{T-1} \gamma^t r^i(\mathbf{s}_t^i, \mathbf{a}_t)\Big]$
$\pi_\psi(\cdot \mid m^i \odot \mathbf{s}_t^i)$	task-conditioned policy based on masked latent states	distribution over $\mathcal{A}$
p_η	skill prior distribution	$\mathbf{z} \sim p_\eta$
$\pi_\varepsilon(\mathbf{a} \mid \mathbf{s}, \mathbf{z})$	skill-conditioned policy	distribution over $\mathcal{A}$
$p(\mathbf{z})$	uniform skill prior on unit hypersphere	$\mathrm{Unif}(\mathbb{S}^{d-1})$
$q_\phi(\mathbf{z} \mid \mathbf{s})$	discriminator for skill identification from states	$\mathcal{S} \to \Delta(\mathcal{Z})$
$\phi_{\text{seg}}(\mathbf{s}_{t+1:t+k}, \mathbf{s}_t)$	segment encoder mapping state segments to embeddings	$\mathbb{R}^{(k+1)\times d_s} \to \mathbb{R}^{d_h}$
$\phi_\xi(\cdot)$	sequence encoder for contrastive learning	trajectories $\to \mathbb{R}^{d_h}$
$\mathcal{L}_{\text{contrast}}^{(n_i)}$	InfoNCE-style contrastive loss for skill discrimination	scalar objective
$\mathrm{d}(\mathbf{x}, \mathbf{x}')$	similarity/distance function between embeddings	$\mathbb{R}^{d_h} \times \mathbb{R}^{d_h} \to \mathbb{R}$
$C_T(\mathcal{D})$	evaluation proxy combining disagreement and reward likelihood	$\mathbb{E}_{(\mathbf{s},\mathbf{a})\sim\mathcal{D}}[\cdot]$
$d_{\text{var}}(\{f_\theta^{(m)}\}_{m=1}^M)$	variance-based disagreement measure across ensemble predictions	$\mathbb{R}^M \to \mathbb{R}$
$f_\theta^{(m)}(\mathbf{s}, \mathbf{a})$	m-th ensemble dynamics model prediction	$\mathcal{S} \times \mathcal{A} \to \mathbb{R}$
Symbol		
$\odot$	Hadamard (element-wise) product	$(\mathbb{R}^d \times \mathbb{R}^d) \to \mathbb{R}^d$
$\mathbb{S}^{d-1}$	$(d-1)$-dimensional unit sphere	$\{\mathbf{z} \in \mathbb{R}^d : \|\mathbf{z}\|_2 = 1\}$

(expandable state space). For each task T_i, we then learn a soft mask $m^i \in (0,1)^{d_i}$ that gates these coordinates and defines the task-specific subspace $m^i \odot \mathbf{s}_t^i$, which we call the MIST states. Thus: (i) *latent factors* are the coordinates of $\mathbf{s}_t^i$, (ii) the *expandable state space* means that the dimensionality d_i can increase across tasks, and (iii) the *masked states* $m^i \odot \mathbf{s}_t^i$ are the subset of those factors that our structure-learning objectives identify as minimal and sufficient for predicting rewards.

Active probing skills To obtain informative data for structure learning, the agent executes *probing skills* parameterized by a latent variable $\mathbf{z}$. We maintain a skill prior $p_\eta(\mathbf{z})$ (e.g., uniform on a hypersphere) and a skill-conditioned exploration policy

$$\mathbf{a}_t \sim \pi_\varepsilon(\cdot \mid \mathbf{s}_t, \mathbf{z}),$$

trained to maximize a mutual-information style objective (Eq. 4) and a contrastive objective (Eq. 5). Rolling out π_ε yields *active probing* that probe how latent factors affect observations and rewards, producing data that is informative for discovering MIST states.

Segment separability Given a latent factor $s_t^{(n)}$ taking values in some space $\mathcal{V}_n$, and a fixed skill $\mathbf{z}$, we consider k-step observation segments

$$\mathbf{o}_{t:t+k}^{(v)} \sim P\big(\mathbf{o}_{t:t+k} \mid s_t^{(n)} = v,\ \pi_\varepsilon(\cdot \mid \cdot, \mathbf{z})\big), \qquad \mathbf{o}_{t:t+k}^{(v')} \sim P\big(\mathbf{o}_{t:t+k} \mid s_t^{(n)} = v',\ \pi_\varepsilon(\cdot \mid \cdot, \mathbf{z})\big),$$

for two distinct values $v \neq v' \in \mathcal{V}_n$. We encode segments with $\mathbf{x}^{(v)} = \phi_\xi(\mathbf{o}_{t:t+k}^{(v)})$ and define *segment separability* via an InfoNCE-style contrastive loss. Skills that induce highly separable segments (low $\mathcal{L}_{\text{contrast}}^{(n)}$) provide strong evidence about the underlying latent factors and are therefore preferred for active probings.

C. Implementation Details on `MIST-WM`

C.1. Mutual Information and Masking Learning

We use MINE (Belghazi et al., 2018) to estimate the mutual information. Following (Wang & Huang, 2025), to avoid instability from inaccurate estimates early in training, the MI weight is annealed from a small value to its target with a cosine schedule:

$$\alpha_{\text{MI}}(t) = \begin{cases} \alpha_{\text{start}} + \frac{1}{2}(\alpha_{\text{end}} - \alpha_{\text{start}})(1 - \cos(\pi t)), & \alpha_{\text{end}} > \alpha_{\text{start}}, \\ \alpha_{\text{end}} + \frac{1}{2}(\alpha_{\text{start}} - \alpha_{\text{end}})(1 + \cos(\pi t)), & \text{otherwise}, \end{cases} \tag{A3}$$

where $t \in [0,1]$ is normalized training time. This smoothly activates the MI constraint and mitigates variance-driven min–max oscillations.

To induce compact latents without the shrinkage artifacts of plain ℓ_1 penalties, we use a modified gated mask inspired by Wang & Huang (2025); Rajamanoharan et al. (2024). The mask is applied to the latent state $\mathbf{s}$; the stochastic component is left unchanged. Let $\mathbf{s}$ denote the latent vector. We define a binary gate and a magnitude reparameterization:

$$\text{Gate:} \quad \mathrm{Gate}(\mathbf{s}) \ := \ \mathbf{1}(\,|\mathbf{s}| + b_{\text{gate}} > 0\,), \tag{A4}$$

$$\text{Magnitude:} \quad f_{\text{mag}}(\mathbf{s}) \ := \ \exp(r_{\text{mag}})\,\mathbf{s} + b_{\text{mag}}, \tag{A5}$$

and the masked latent is

$$\boldsymbol{m} \odot \mathbf{s} \ := \ \mathrm{Gate}(\mathbf{s}) \ \odot \ f_{\text{mag}}(\mathbf{s}). \tag{A6}$$

We couple this with an adaptive sparsity objective on the gate:

$$\mathcal{L}_{\ell_1}(\boldsymbol{m}) \ = \ \big\|\mathrm{ReLU}\big(\mathrm{Gate}(\mathbf{s})\big)\big\|_1, \tag{A7}$$

where the target sparsity threshold is increased smoothly using the cosine schedule in equation A3. This schedule provides fine-grained control over the active fraction of latent dimensions while preserving exploration efficiency.

C.2. Details on Skill Library Learning

We use DIAYN (Eysenbach et al., 2019) and METRA (Park et al., 2024) as our skill library learning framework.

For DIAYN, let $z \sim p_\eta(z)$ be a skill sampled per episode/segment and $s \sim d^{\pi_\psi}(\cdot \mid z)$ the (discounted) state distribution induced by the skill–conditioned policy $\pi_\psi(a \mid s, z)$. Define

$$\mathcal{F}(\psi, \eta) \;=\; \underbrace{\mathcal{H}[A \mid S, Z]}_{\text{max-ent exploration under skills}} \;-\; \mathcal{H}[Z \mid S] \;+\; \mathcal{H}[Z], \tag{A8}$$

where entropies are taken under $z \sim p_\eta$, $s \sim d^{\pi_\psi}(\cdot \mid z)$, and $a \sim \pi_\psi(\cdot \mid s, z)$. Expanding the KL terms gives

$$\mathcal{F}(\psi, \eta) = \mathcal{H}[A \mid S, Z] + \mathbb{E}_{z \sim p_\eta,\, s \sim d^{\pi_\psi}(\cdot \mid z)}\big[\log p(z \mid s)\big] - \mathbb{E}_{z \sim p_\eta}\big[\log p_\eta(z)\big]. \tag{A9}$$

Using a variational classifier $q_\phi(z \mid s)$, we obtain the tractable lower bound

$$\mathcal{F}(\psi, \eta) \;\geq\; \mathcal{G}(\psi, \eta, \phi) \;:=\; \mathbb{E}_{z \sim p_\eta,\, s \sim d^{\pi_\psi}(\cdot \mid z)}\Big[\underbrace{\mathcal{H}\big(\pi_\psi(\cdot \mid s, z)\big)}_{\text{entropy of } \pi} + \log q_\phi(z \mid s) - \log p_\eta(z)\Big]. \tag{A10}$$

For METRA, we consider the skill reward as:

$$r_\phi(\mathbf{s}, \mathbf{z}, s\mathrm{v}') = \big(\phi(\mathbf{s}') - \phi(\mathbf{s})\big)^\top \mathbf{z}. \tag{A11}$$

and the total objective is then as:

$$\mathcal{L}_{\text{METRA}}(\phi, \lambda) = \mathbb{E}_{(\mathbf{s}, \mathbf{z}, \mathbf{s}') \sim \mathcal{D}}\Big[\big(\phi(\mathbf{s}') - \phi(\mathbf{s})\big)^\top \mathbf{z} + \lambda \,\mathrm{clip}_\varepsilon\big(1 - \|\phi(\mathbf{s}') - \phi(\mathbf{s})\|_2^2\big)\Big], \quad \lambda \geq 0. \tag{A12}$$

Both are optimized using SAC (Haarnoja et al., 2018) to learn the exploration policy. Hyperparameters are given in Section D.3.

C.3. Details on Curriculum Learning

We follow a UED-style scheduler for environment selection. At each step, we compute an ensemble-disagreement proxy Δ_T (model-error hardness) per environment from its buffer:

$$\Delta_T \;=\; \mathbb{E}_{(s,a) \sim \mathcal{B}_T}\big[\mathrm{Tr}\big(\mathrm{Cov}_{m=1}^{M}\,[\, f_{\theta^{(m)}}(s, a)\,]\big)\big]\,. \tag{A13}$$

We then normalize scores before sampling:

$$\tilde{\Delta}_T \;=\; \frac{\Delta_T - \min_{T'} \Delta_{T'}}{\max_{T'} \Delta_{T'} - \min_{T'} \Delta_{T'} + \varepsilon}. \tag{A14}$$

A Boltzmann distribution with temperature η emphasizes harder environments:

$$p_\eta(T) \;=\; \frac{\exp\big(\tilde{\Delta}_T / \eta\big)}{\sum_{T' \in \mathcal{T}} \exp\big(\tilde{\Delta}_{T'} / \eta\big)}. \tag{A15}$$

Then, we mix domain randomization with error-driven selection: with probability p_{DR} (or if any $\mathcal{B}_T$ is empty), we sample environment parameters at random; otherwise, we sample according to p_η:

$$u \sim \mathcal{U}[0, 1], \qquad T_{\text{next}} \sim \begin{cases} \mathrm{DomainRandomisation}(\Theta), & \text{if } u < p_{\mathrm{DR}} \text{ or } \exists\, T : \; |\mathcal{B}_T| = 0, \\ \mathrm{Cat}\big(p_\eta(\cdot)\big), & \text{otherwise.} \end{cases} \tag{A16}$$

To compute the disagreement term, we use an ensemble of transition functions $f_\theta(\mathbf{s}, \mathbf{a})$ corresponding to the RSSM dynamics in the Dreamer model, following Ball et al. (2020); Sekar et al. (2020); Mendonca et al. (2021). Concretely, we train an ensemble of one-step predictors that map the current model state and action to the next model state. The ensemble is optimized jointly with the world model on latent transitions $\mathbf{s}' \sim p_\theta(\mathbf{s}' \mid \mathbf{s}, \mathbf{a})$, as defined in Eq. 1.

C.4. Expandable Latent Space

When transitioning from task T_i to T_{i+1}, we allow the latent dimensionality to grow, $d_{i+1} > d_i$. We follow a simple over-parameterized heuristic that is consistent with practice and then rely on structure learning to select the task-relevant subspace. For each benchmark we initialize the Dreamer latent dimensionality d_1 to a fixed value and keep it shared across tasks at the beginning (e.g., $d_1 = 512$ for Meta-World, RoboSuite, and Kitchen, which have high-dimensional visual observations, and $d_1 = 256$ for DMControl). When moving from task T_i to T_{i+1}, we allow the latent dimensionality to grow by a fixed increment, $d_{i+1} = d_i + \Delta d$. where we set $\Delta d = 32$ in all experiments. The choice of d_1 and Δd is therefore a heuristic design decision rather than an oracle choice of the "correct" dimension. In practice, this slight over-parameterization is benign because our structure-learning module (through the sufficiency and minimality objectives and the learned mask m^i) identifies and uses only the task-relevant subset of dimensions (the MIST states), while irrelevant coordinates are effectively suppressed.

Concretely, we fine-tune the encoder and RSSM parameters up to the latent layer for T_i and adapt the final linear layer that maps the encoder/RSSM features into $\mathbb{R}^{d_{i+1}}$. The additional $d_{i+1} - d_i$ coordinates are initialized randomly and trained for T_{i+1}. The decoders (observation, reward, and continuation) are similarly extended to read the expanded latent vector, but we fine-tune their parameters for the first d_i dimensions and learn the additional weights for the new coordinates.

C.5. Algorithmic Frameworks

Algorithm 1 gives the full algorithm of `MIST-WM`.

C.6. Additional Details on Representation Learning Components

Unstructured Latent States. The Dreamer world model produces latent states $\mathbf{s}_t \in \mathbb{R}^d$ through the RSSM encoder $q_\theta(\mathbf{s}_t \mid \mathbf{o}_t, h_t, \mathbf{a}_{t-1})$. These latents are *unstructured*: no constraints are imposed on their factorization, and all coordinates may encode arbitrary mixtures of task-relevant and task-irrelevant features. During structure learning, the encoder parameters generating $\mathbf{s}_t$ remain **frozen** so that all subsequent structure-learning objectives operate over a fixed latent basis.

Structure Learning. Given the unstructured latents $\mathbf{s}_t$, we identify a structured subspace $_i^{\min}$ for each task T_i via a learnable mask $m^i \in (0,1)^d$ and two task-specific objectives (Eq. 2 & Eq. 3). During this stage, the RSSM encoder and Dreamer dynamics are **frozen**; only the mask m^i and the MI estimator parameters receive gradients.

MIST States. For each task T_i, the MIST representation is defined as

$$\tilde{\mathbf{s}}_t^i = m^i \odot \mathbf{s}_t^i \in_i^{\min},$$

which retains only the coordinates necessary for reward prediction and decision making. Policies and value functions $\pi_\psi(\mathbf{a}_t \mid \tilde{\mathbf{s}}_t^i)$ operate exclusively on this subspace, and gradients through RL losses $\nabla_\psi^{(i)}{}_{\mathrm{RL}}(\psi)$ do not update the world model.

Active Probing Skills. When encountering a new task, the agent collects informative trajectories via latent skills $\mathbf{z} \sim p_\eta(\mathbf{z})$. Actions follow a skill-conditioned policy $\pi_\varepsilon(\mathbf{a}_t \mid \mathbf{s}_t, \mathbf{z})$, trained using the mutual-information based MISL objective (Eq. 4). Here only the skill policy η and discriminator q_ϕ receive gradients; the world model and encoders stay **fixed** during skill learning.

Segment Separability. To select informative skills, we measure how distinguishable two segments generated from different latent-factor values are. Let $\mathbf{o}_{t:t+k}^{(v)}$ and $\mathbf{o}_{t:t+k}^{(v')}$ be observation segments produced under skill $\mathbf{z}$. After encoding them using ϕ_ξ, we apply an InfoNCE objective (Eq. 5). Gradients update the segment encoder ϕ and the skill parameters ε.

Table A2 summarizes which objectives update which components.

C.7. Evaluation on the Learned Representations

As illustrated in Fig. 4, we assess representation quality by measuring how well the learned latents predict the ground-truth simulator factors. Since the latent space can be over-parameterized, a single factor may be encoded across multiple

Module	WM Loss	Structure Losses	Skill Losses
Dreamer encoder / RSSM	✓	frozen	frozen
Reward / obs decoders	✓	✓	frozen
Mask m^i	frozen	✓	frozen
MI estimator (MINE)	frozen	✓	frozen
Skill policy ε	frozen	frozen	✓
Skill discriminator q_ϕ	frozen	frozen	✓
Segment encoder ϕ_ξ	frozen	frozen	✓
Policy / value ψ	frozen	frozen	✓(RL)

Table A2. Summary of gradient flow across modules. A checkmark indicates parameters updated under the corresponding losses.

coordinates. We therefore first fix all model parameters and only use the encoders to map observations to latent vectors $\mathbf{s}_t^i$, so that no further learning happens in the world models during this evaluation.

Given the assignment of latent dimensions to each ground-truth variable, we group the corresponding coordinates and attach a separate probe network to every group. Each probe is a two-layer MLP with hidden size 128, trained to regress all ground-truth factors associated with that group, and we report the coefficient of determination (R^2) between the predictions and the true values.

To train the probes, we randomly split the evaluation rollouts into two parts: 40% of the data is used to fit the MLPs and the remaining 60% is held out for computing the correlation metrics. The rollouts themselves are obtained by sampling random configurations of the underlying ground-truth latent factors. We use MSE loss for continuous variables and cross entropy loss for categorical variables.

After training the MLPs, we use the coefficient of determination (R^2) to determine the "matching quality" of learned representation and the ground-truth ones. The R^2 coefficient quantifies how well the predicted values $\hat{x}_i$ explain the variance of a ground-truth variable x_i. For continuous variables, it is defined as

$$R^2 = 1 - \frac{\sum_i (x_i - \hat{x}_i)^2}{\sum_i (x_i - \bar{x})^2}, \tag{A17}$$

where $\bar{x} = \frac{1}{N}\sum_i x_i$ denotes the empirical mean of the ground-truth values. Similarly, for categorical variables, we can use the most frequent category in the dataset to approximate $\bar{x}$, and then measure the distance by equal: $\delta_{x_i = \hat{x_i}}$.

D. Details on Task Settings and Hyperparameters

D.1. Task Settings

We evaluate our framework across a diverse set of standard continuous control (locomotion) and robotic manipulation benchmarks. From DMControl (Tunyasuvunakool et al., 2020), we consider three representative locomotion tasks—*Cheetah Run*, *Walker*, and *Reacher*. To assess manipulation and generalization, we further include Meta-World (Yu et al., 2020), a widely used multi-task benchmark covering diverse object-centric skills, and extend to more realistic robotic platforms such as Franka-Kitchen (Gupta et al., 2019) and Robosuite (Zhu et al., 2020).

D.1.1. Benchmarks

DMControl The DeepMind Control Suite (DMControl) (Tunyasuvunakool et al., 2020) is a standard continuous-control benchmark based on MuJoCo physics. We evaluate on three representative tasks:

- Cheetah-Run: a planar cheetah agent optimized for speed, testing fast locomotion and stability.
- Walker: a bipedal agent balancing and walking forward, emphasizing coordination.
- Reacher: a 2-link arm reaching for randomly placed targets, measuring precise control and sample efficiency.

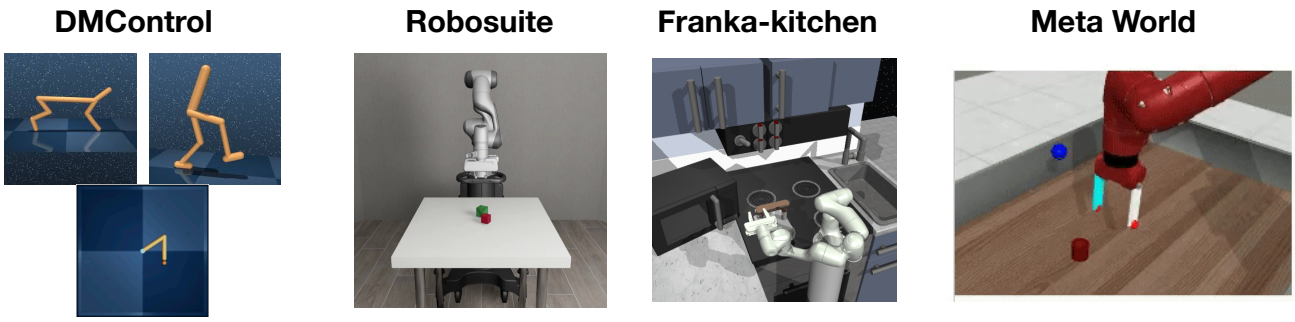

Figure A1. Visualization on tested benchmarks.

Meta-World Meta-World (Yu et al., 2020) is a large multi-task benchmark for robotic manipulation. Each task involves a 7-DoF robotic arm manipulating the same object but with opposite goals, providing an ideal testbed for multi-task interference.

Franka-kitchen The Franka-Kitchen benchmark (Gupta et al., 2019) simulates a realistic Franka Emika Panda robot arm interacting with common kitchen appliances (microwave, lights, burners, cabinets). Tasks are composed from multiple sub-goals, requiring long-horizon planning, object interaction, and compositional skill reuse.

Robosuite Robosuite (Zhu et al., 2020) is a suite of MuJoCo-based robotic benchmarks designed for general-purpose robot learning. It provides a diverse set of manipulation tasks with realistic object dynamics and robot arms (including Sawyer and Panda).

D.1.2. Single Task Learning

We evaluate single-task learning across four suites. In **DMControl**, we use *Cheetah Run*, *Walker*, and *Reacher*. In **Meta-World**, we use *Box-Close*, *Lever-Pull*, *Assembly*, *Bin-Picking*, *Handle-Pull*, *Door-Unlock*, *Faucet-Close*, and *Drawer-Open*. In **RoboSuite**, we use *Lift* and *Pick & Place*. In **Franka Kitchen**, we use *Microwave*, *Kettle*, *Stove*, *Light*, and *Cabinet*.

We train for 10^6 environment steps on DM Control, 5×10^6 on Meta-World, 5×10^6 on RoboSuite, and 5×10^4 on Franka Kitchen.

D.1.3. Generalization tasks

Skill generalization. For **RoboSuite**, we evaluate stacking tasks that can be composed from skills learned on *Lift* and *Pick & Place*. For **Franka Kitchen**, we transfer previously learned skills to long-horizon sequences using the extended setup from (Chen et al., 2024). We consider two multi-task sequences: **MT-1**: *turn on microwave* $\rightarrow$ *move kettle* $\rightarrow$ *turn on stove* $\rightarrow$ *turn on light*; **MT-2**: *turn on microwave* $\rightarrow$ *turn on stove* $\rightarrow$ *turn on light* $\rightarrow$ *slide cabinet to the right*. We use 10^6 adaptation steps for RoboSuite and 1.25×10^5 for Franka Kitchen.

Compositional & unseen generalization. For **Meta-World**, we test compositional generalization to *door-open* and *drawer-close*, and unseen-task generalization to *coffee-push*, *sweep-into*, *push-wall*, *reach-wall*, and *plate-slide* (randomly selected). All adaptations use 2.3×10^5 environment steps.

D.2. Environment Settings

RoboSuite. We design controlled multi-object scenes to encourage recovery of system variables and enable active probings. Each episode initializes *three* cubes, with two cubes sharing identical color and texture. We construct a bank of ten environment variants that systematically vary a single physical factor at a time—(i) mass (`body_mass`), (ii) friction coefficients, and (iii) orientation components (e.g., Euler angles)—while keeping all other factors fixed. Within any episode, only *two* of the three cubes differ along the currently controlled factor. This parametrization yields clear probing targets and facilitates learning an active probing policy.

Meta-World & Franka Kitchen. Given the more limited low-level control in *Meta-World*, we adopt multi-object settings

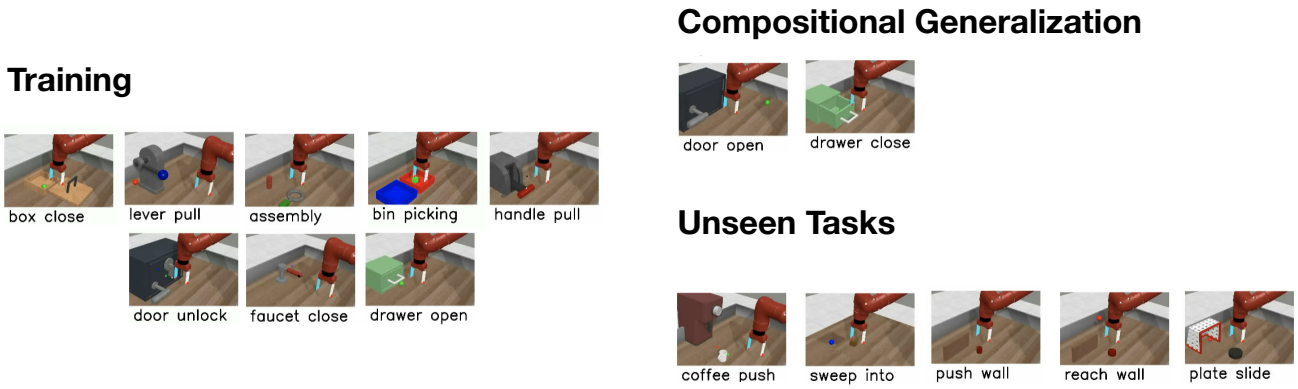

Figure A2. Visualization on the tasks used for compositional generalization and unseen tasks.

analogous to *Franka Kitchen*, which naturally contains diverse, manipulable objects. For Meta-World, we reuse the *Continual Bench* setup from (Liu et al., 2025) to explore environments featuring drawers, doors, boxes, bins, and handles, in order to learn object-centric latent representations before downstream tasks. All baselines are granted the same phase-one interaction protocol and budget to ensure fairness. Unless otherwise specified, we allocate 10% of the total environment steps for this representation-learning phase across suites.

D.3. Hyperparameters

We build on the official *Dreamer-v3* codebase (including *DMControl*/MuJoCo tasks). For *Meta-World*, we adopt the Dreamer-v3 hyperparameters as specified in the *TD-MPC2* paper. For *Franka Kitchen* and *RoboSuite*, we use the same configuration as Meta-World due to task similarity. Baseline implementations follow their public releases wherever possible: *DINO-WM* is based on its official learning setup, but we replace the original MPC component with either PPO or SAC to match our environments; *TD-MPC2* is run with its original settings on *DMControl*. Beyond these, our method introduces phase-specific hyperparameters for (i) the exploration policy, (ii) MIST learning, and (iii) adaptation. The specification for (i) - (iii) is provided in Table A4-A5. The hyperparameters of SAC and PPO are specified in Table A6-A7.

D.4. Details on Computational Requirements

All experiments are conducted on 4 NVIDIA A100 GPUs with 80GB memory. We report the training cost in GPU days and compare against the base model (Dreamer-v3). As shown in Table A3, our method requires slightly more compute while achieving better generalization.

Table A3. Training cost (GPU days) comparison with Dreamer-v3 on different suites.

Task Suite	Ours	Dreamer-v3
DM Control	0.35	0.25
Meta-World	0.75	0.50
Franka Kitchen	0.35	0.30
RoboSuite	0.75	0.60

E. Full Results

E.1. Full Results on Representation Probing

Table A9 reports the full representation–probing results; the averaged scores appear in Fig. 4(c) of the main paper. The trends mirror our main findings. `MIST-WM` achieves the best overall performance. In the yellow block (exploration skills), METRA is consistently second-best. In the green block (world models), factored approaches (*I-Factor* and *Denoised MDP*) outperform DINO-WM on average. Notably, DINO-WM excels on the *size* factor, likely due to its strong pretrained visual prior.

Table A4. Agent probing exploration and world model hyperparameters for `MIST-WM`.

Hyperparameter	Value
General	
Batch size	128 (DMControl); 512 (Others)
Ratio of imagined samples	0.5 (DMControl); 0.2 (Others)
Replay buffer size	10^6 (DMControl); 10^5 (Others)
Active Probing	
Learning rate	0.0001
Replay buffer size	10^6 (DMControl); 10^5 (Others)
Contrastive encoder layers	3
Contrastive hidden units	256
Episodes per batch	16 (DMControl); 32 (Others)
Discount factor γ	0.99
Policy network layers	2
Policy network hidden units	1024
Gradients per episode	50 (DMControl); 100 (Others)
MISL algorithm	DIAYN (DMControl); METRA (Others)
Target smoothing coef.	0.995
Entropy coef.	0.01
World Model	
Dreamer deterministic size	512 for Meta World, 256 for Others
Dreamer stochastic size	16
Reward prediction layers	2
Reward pred. hidden units	256 (DMControl); 512 (Others)
Policy network layers	3
Policy net hidden units	256 (DMControl); 512 (Others)
Minimal score coef.	10^{-3} (DMControl); 10^{-2} (Others)
Sufficiency score coef.	10^{-3} (DMControl); 10^{-2} (Others)

E.2. Full Results on Single Task Learning

Fig. A3 presents the complete single-task learning results, covering 8 tasks from Meta-World and 3 tasks from DMControl, complementing the summary shown in Fig. 5.

E.3. Full Results on Generalization Tasks

Figs. A5 shows the complete results on skill generalization and on compositional/unseen tasks, respectively. The summary results are given in Fig. A4.

E.4. Full Results on Ablation Studies

Fig. A6 gives the full results on ablation studies, and the summary results are given in Fig. 7 in the main paper.

Discussion: Choice of Skill-Learning Baselines. In the ablation studies, our primary goal is to examine how replacing our probing skill module with different unsupervised skill-learning methods affects overall performance. While the original experiments used METRA as a representative baseline, we have additionally included DIAYN following the reviewer's suggestion. Table A12 summarizes the performance across three representative settings (single-task, multi-task, and compositional generalization). We find that METRA generally outperforms DIAYN, both as a standalone skill-learning algorithm and when used as the skill-library initializer for MIST-WM. However, we emphasize that the choice between METRA and DIAYN is not central to our framework: both are only used to initialize the skill library, while the probing skills are subsequently refined using our separability objective in Eq. 5. As a result, MIST-WM remains largely agnostic to the choice of initial skill-learning algorithm.

Table A5. Training, adaptation, and curriculum hyperparameters for MIST-WM.

Hyperparameter	Value
Training	
Training steps	5×10^6 (MW, RS); 5×10^4 (Kitchen); 10^6 (DMControl)
Maximize MINE after	10% of total steps
Adaptation	
Adaptation steps	2.3×10^5 (Meta-World)
Sparsity	0.35
Maximize MINE (start)	0

Hyperparameter	Value
Batch size	128 for Robsouite, 256 for Meta-World
Network architecture	MLPs
Actor / critic size	3 fully connected layers with 256 units
Non-linearity	ReLU
Policy initialization	Standard Gaussian
Policy learning rate	3×10^{-4}
Optimizer	Adam
Adam β (policy)	$(0.9, 0.999)$
Adam β (Q-function)	$(0.9, 0.999)$
Discount	0.99

Table A6. SAC hyperparameters for Meta-World and RoboSuite.

Parameter	Value
Network architecture	MLPs
Actor / critic size	3×256 units for DMC, 3×400 units for Kitchen
Non-linearity	ReLU
Observation normalization	Yes
Reward normalization	Yes
Reward clipping (stddev.)	10
Batch size	128
Policy trust region	0.2
Value trust region	No
Advantage normalization	Yes
Entropy penalty scale	0.01
Discount factor	0.997
GAE λ	0.95
Learning rate	3×10^{-4}
Gradient clipping	0.5
Adam ε	10^{-5}

Table A7. PPO hyperparameters for DMC and Kitchen.

Table A8. Curriculum learning hyperparameters.

Hyperparameter	Value
Temperature η	0.1
Domain randomization prob. p_{DR}	0.3
Normalization constant ε	10^{-6}
Ensemble size M	5

Algorithm 1 MIST-WM

Require: Task set $\{T_i\}_{i=1}^N$, environments $\{\mathcal{E}_i\}_{i=1}^N$, world-model parameters θ, policy parameters ψ, exploration policy $\pi_\varepsilon(\mathbf{a} \mid \mathbf{s}, \mathbf{z})$, skill prior $p_\eta(\mathbf{z})$, curriculum buffer $\{C_T(D_i)\}_{i=1}^N$

0: Initialize replay buffers $D_i \leftarrow \emptyset$ for all i
0: Initialize world model θ, task-specific masks $\{m_i\}$, MI estimator, and policy ψ
0: Pretrain skill library (MISL) by maximizing Eq. 4 on randomly sampled environments to obtain $\pi_\varepsilon(\mathbf{a} \mid \mathbf{o}, \mathbf{z})$

Outer loop over curriculum

0: **for** training iteration $k = 1, 2, \ldots$ **do**
0: For each task T_i, compute difficulty proxy

$$C_T(D_i) \leftarrow \mathbb{E}_{(s,a,r)\sim D_i}\Big[\mathrm{Var}_m\big(f_\theta^{(m)}(\mathbf{s}, \mathbf{a})\big) - \log p_\theta(r \mid \mathbf{s}, \mathbf{a})\Big]$$

0: Select next task by worst-case error: $i^\star \leftarrow \arg\max_i C_T(D_i)$
0: Reset environment to $\mathcal{E}_{i^\star}$

Active probing and data collection on $T_{i^\star}$

0: **for** $e = 1$ to N_{int} **do**
0: Sample a skill $\mathbf{z} \sim p_\eta(\mathbf{z})$
0: Roll out skill-conditioned exploration policy $\mathbf{a}_t \sim \pi_\varepsilon(\mathbf{a} \mid \mathbf{s}_t, \mathbf{z})$ for H steps in $\mathcal{E}_{i^\star}$
0: Collect transitions $(\mathbf{o}_t, \mathbf{a}_t, r_t, \mathbf{o}_{t+1})_{t=0}^{H-1}$ and compute its contrastive score according to Eq. 5
0: Update π_ϵ using Eq. 4
0: **end for**
0: Update π_ϵ using Eq. 5 on collected segments to favor skills with high information gain
0: With high probability p, store segments among the top-k scores into $D_{i^\star}$, and $1-p$ to store the remaining segments

World model and policy learning with MIST objectives on $T_{i^\star}$

0: **for** $u = 1$ to N_{wm} **do**
0: Sample a minibatch of sequences from $D_{i^\star}$
0: Encode $\mathbf{o}_{0:T}^{i^\star}$ and $\mathbf{a}_{0:T}^{i^\star}$ with p_θ to obtain $\mathbf{s}_{0:T}^{i^\star}$ and recurrent states $\mathbf{h}_{0:T}^{i^\star}$
0: Compute Dreamer-based loss $\mathcal{L}_{\text{WM}}^{(i^\star)}(\theta)$ as in Eq. 1
0: Compute task-specific sufficiency score

$$R_{\text{suff}}^{(i^\star)}(\theta) = \mathbb{E}\Big[\sum_{t=0}^{T-1} \log p_\theta(r_t^{i^\star} \mid m_{i^\star} \odot \mathbf{s}_t^{i^\star}, \mathbf{a}_t)\Big]$$

0: Estimate mutual information term $MI(m_{i^\star} \odot \mathbf{s}_{1:T}^{i^\star}, g_{i^\star})$ using MINE and minimality score

$$R_{\text{min}}^{(i^\star)}(\theta) = MI(m_{i^\star} \odot \mathbf{s}_{1:T}^{i^\star}, g_{i^\star}) - \lambda_M \|m_{i^\star}\|_1$$

0: Update θ, $m_{i^\star}$, and MI-estimator parameters by minimizing

$$\mathcal{L}_{\text{total}}^{(i^\star)} = \mathcal{L}_{\text{WM}}^{(i^\star)} - \alpha_{\text{suff}} R_{\text{suff}}^{(i^\star)} - \alpha_{\text{min}} R_{\text{min}}^{(i^\star)}$$

0: **end for**
0: **for** $u = 1$ to N_{rl} **do**
0: Sample trajectories from $D_{i^\star}$ and encode them to latent states $\mathbf{s}_t^{i^\star}$
0: Form task-specific MIST representation $\tilde{\mathbf{s}}_t^{i^\star} = m_{i^\star} \odot \mathbf{s}_t^{i^\star}$
0: Update policy $\pi_\psi(\mathbf{a} \mid \tilde{\mathbf{s}}_t^{i^\star})$ to maximize $J_{\text{RL}}^{(i^\star)}(\psi) = \mathbb{E}\Big[\sum_{t=0}^{T-1} \gamma^t r_t^{i^\star}\Big]$
0: Roll out the updated policy π_ψ in $\mathcal{E}_{i^\star}$ for H steps to obtain new trajectories τ_{new}
0: Add τ_{new} into $D_{i^\star}$ and update θ using minibatches sampled from $D_{i^\star} \cup \tau_{\text{new}}$
0: **end for**

Update curriculum statistics

0: Recompute $C_T(D_{i^\star})$ with the updated θ
0: **end for**=0

Table A9. **Probing results (R^2) under different settings**. The pink region corresponds to varying the exploration data using different collection methods, while the green region corresponds to varying the world-modeling methods while keeping the data fixed. The average is computed across all factors excluding the size.

Methods	Size	C-pos	C-Orient	G-pos	G-orient	G-openness	C-Mass	Average
Random	0.01	0.92	0.16	0.48	0.21	0.06	0.03	0.31
METRA	0.03	0.95	0.85	0.51	0.49	0.20	0.55	0.59
Curiosity Replay	0.02	0.96	0.53	0.23	0.36	0.15	0.39	0.44
Plan2Explore	0.01	0.93	0.59	0.41	0.26	0.10	0.40	0.45
DINO-WM	**0.76**	0.75	0.09	0.53	0.42	0.00	0.61	0.40
I-Factor	0.00	0.79	0.41	0.56	0.47	0.08	0.59	0.48
Denoised MDP	0.00	0.83	0.30	0.72	0.65	0.16	0.68	0.56
`MIST-WM`	0.02	**1.00**	**0.94**	**0.86**	**0.69**	**0.21**	**0.96**	**0.78**

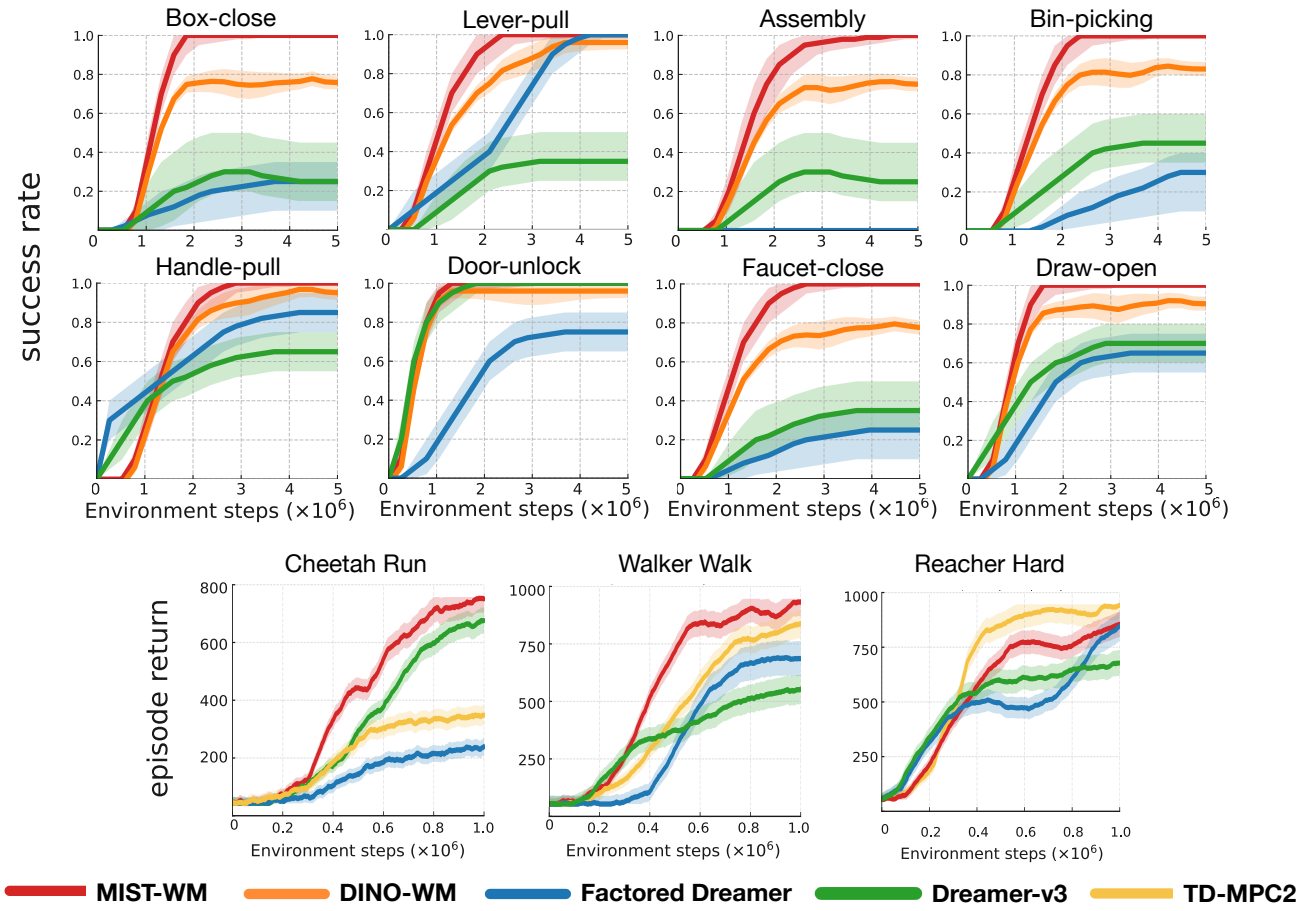

Figure A3. Results (across 5 seeds) on single-task learning, including **robotic manipulation** tasks (Meta World) and **locomotion** (DMControl).

Table A10. Success rate at 2M environment steps (mean ± std over 5 seeds).

Environment	Ours	DINO-WM	Factored Dreamer	Dreamer-v3	TD-MPC2
Box-close	**0.94** ± 0.02	0.75 ± 0.05	0.15 ± 0.06	0.26 ± 0.13	0.09 ± 0.02
Lever-pull	**0.91** ± 0.05	0.72 ± 0.04	0.38 ± 0.08	0.29 ± 0.11	0.06 ± 0.03
Assembly	**0.79** ± 0.12	0.61 ± 0.03	0.06 ± 0.02	0.22 ± 0.08	0.12 ± 0.06
Bin-picking	**0.88** ± 0.05	0.71 ± 0.04	0.10 ± 0.06	0.31 ± 0.12	0.08 ± 0.03
Handle-pull	**0.84** ± 0.06	0.80 ± 0.02	0.61 ± 0.09	0.53 ± 0.08	0.15 ± 0.04
Door-unlock	0.96 ± 0.02	0.91 ± 0.04	0.55 ± 0.08	**0.98** ± 0.05	0.13 ± 0.02
Faucet-close	**0.91** ± 0.06	0.68 ± 0.08	0.23 ± 0.12	0.18 ± 0.11	0.10 ± 0.04
Draw-open	**0.97** ± 0.02	0.86 ± 0.04	0.62 ± 0.09	0.54 ± 0.08	0.17 ± 0.05

Table A11. DMControl performance at 1M steps (mean ± std).

Environment	Ours	DINO-WM	Factored Dreamer	Dreamer-v3	TD-MPC2
Cheetah-Run	**731.6** ± 32.9	165.2 ± 41.8	217.5 ± 16.4	661.0 ± 42.3	339.8 ± 31.6
Walker-Walk	**904.2** ± 42.5	286.5 ± 37.4	557.2 ± 56.4	698.2 ± 52.5	867.5 ± 51.2
Reacher-Hard	871.6 ± 38.5	346.2 ± 29.8	869.3 ± 33.9	702.4 ± 43.3	**915.6** ± 23.3

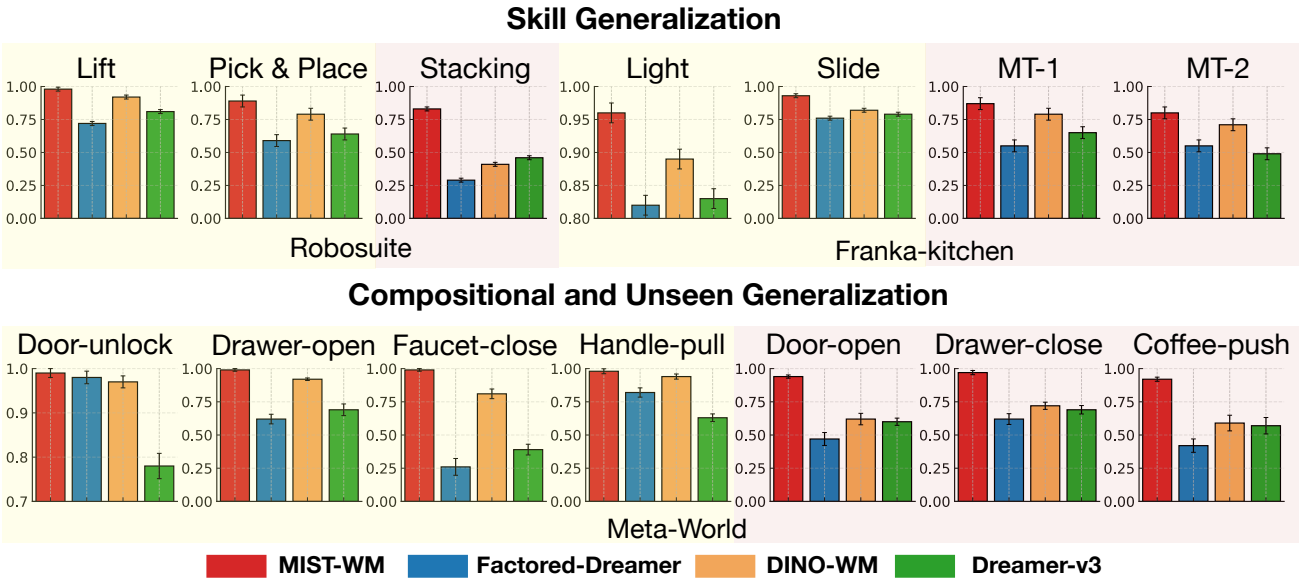

Figure A4. Success rate (across 5 seeds) on skill and compositional generalization, including tasks in Robosuite, Franka-kitchen, and Meta-World. Results in light yellow boxes are those on source tasks, and light pink are those on generalization tasks. Error bars indicate the standard deviation.

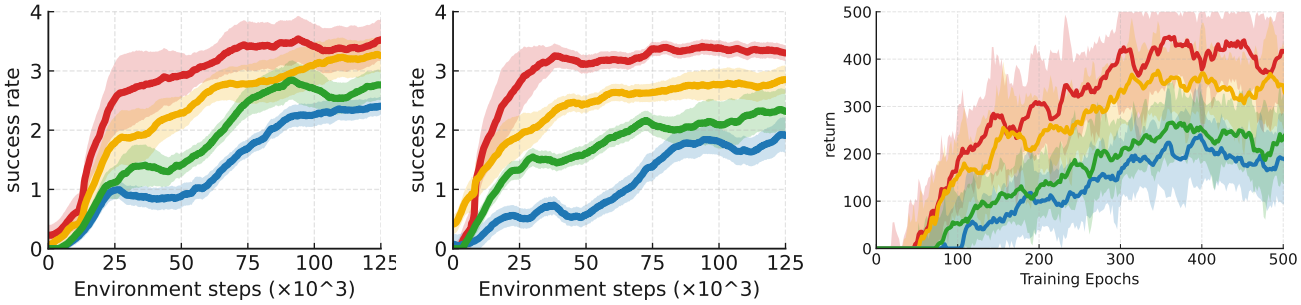

Figure A5. Results (across 5 seeds) on skill generalization tasks, where the left two figures are the skill generalization curves on Franka Kitchen MT-1 and MT-2; and the right figure is the generalization results on robosuite-stacking. The yellow curve indicates the results using DINO-WM.

Table A12. Ablation comparing METRA and DIAYN as skill-library initializers.

Environment	Ours (METRA)	Ours (DIAYN)	METRA	DIAYN	Curious Replay
Cheetah	$\mathbf{741.0 \pm 25.6}$	731.6 ± 32.9	680.8 ± 32.3	664.5 ± 39.6	635.8 ± 46.8
Box-close	$\mathbf{0.94 \pm 0.02}$	0.79 ± 0.04	0.81 ± 0.06	0.59 ± 0.10	0.48 ± 0.12
Coffee-push	$\mathbf{0.89 \pm 0.05}$	0.82 ± 0.03	0.76 ± 0.07	0.62 ± 0.05	0.30 ± 0.16

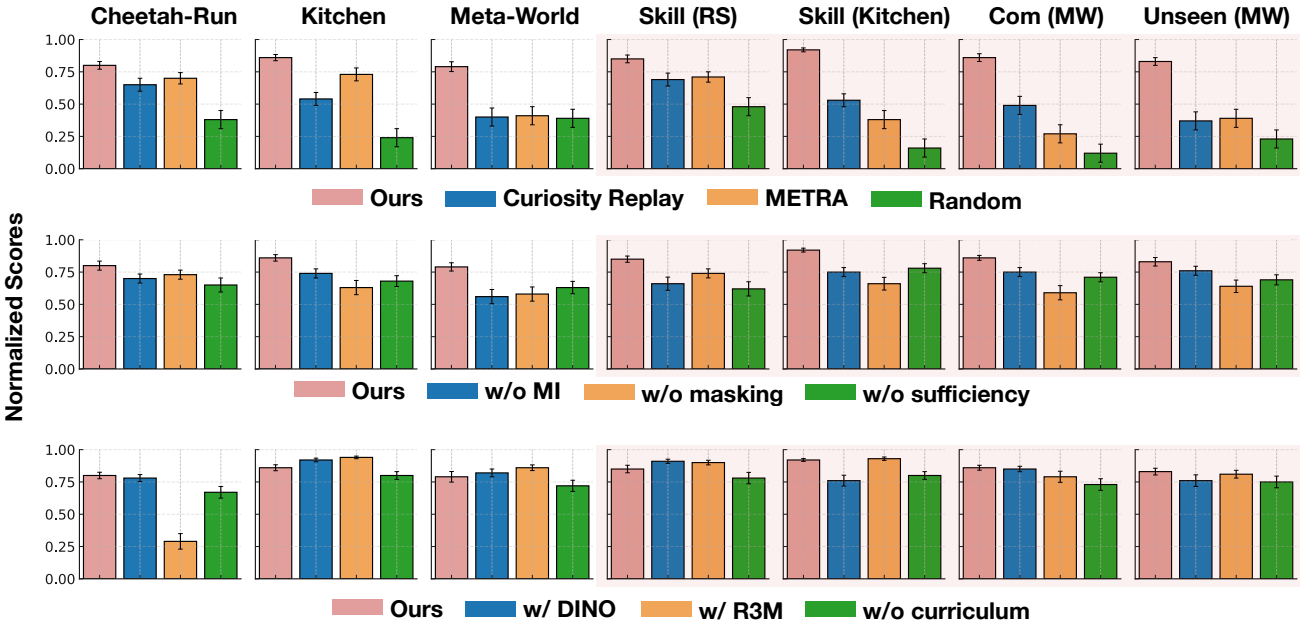

Figure A6. **Ablation studies. Row 1—Exploration policy:** compare our skill-conditioned exploration against *Random*, *Intrinsic motivation* (Curiosity Replay), and *MISL* (METRA). **Row 2—Structure-learning terms:** remove the MI term in the *minimality* score (w/o MI), remove *masking* in the minimality score (w/o Mask), and remove the *sufficiency* term (w/o Suff). **Row 3—Backbones and curriculum:** replace our backbone with *DINO-WM* or *R3M*, and evaluate w/o curriculum. Error bars indicate the standard deviation.